catalysts

MDPI

Review

Controlling Redox Enzyme Orientation at Planar Electrodes

Vivek Pratap Hitaishi [1], Romain Clement [1], Nicolas Bourassin [2], Marc Baaden [2], Anne de Poulpiquet [1], Sophie Sacquin-Mora [2], Alexandre Ciaccafava [3] and Elisabeth Lojou [1,*]

[1] National Center for Scientific Research (CNRS), Aix Marseille University, BIP, UMR 7281, 31 Chemin Aiguier, 13009 Marseille, France; vhitaishi@imm.cnrs.fr (V.P.H.); rclement@imm.cnrs.fr (R.C.); adepoulpiquet@imm.cnrs.fr (A.d.P.)

[2] Laboratoire de Biochimie Théorique, National Center for Scientific Research (CNRS), UPR9080, Université Paris Diderot, Sorbonne Paris Cité, PSL Research University, 13 rue Pierre et Marie Curie, 75005 Paris, France; bourassin@ibpc.fr (N.B.); baaden@ibpc.fr (M.B.); Sophie.Sacquin-Mora@ibpc.fr (S.S.-M.)

[3] Chemistry and Biology of Membranes and Nanoobjects, UMR 5248 CNRS, University of Bordeaux, Bat. B14 allée Geoffroy St. Hilaire, 33600 Pessac, France; a.ciaccafava@cbmn.u-bordeaux.fr

* Correspondence: lojou@imm.cnrs.fr; Tel.: +33-4-91-16-41-44

Received: 13 April 2018; Accepted: 28 April 2018; Published: 4 May 2018

Abstract: Redox enzymes, which catalyze reactions involving electron transfers in living organisms, are very promising components of biotechnological devices, and can be envisioned for sensing applications as well as for energy conversion. In this context, one of the most significant challenges is to achieve efficient direct electron transfer by tunneling between enzymes and conductive surfaces. Based on various examples of bioelectrochemical studies described in the recent literature, this review discusses the issue of enzyme immobilization at planar electrode interfaces. The fundamental importance of controlling enzyme orientation, how to obtain such orientation, and how it can be verified experimentally or by modeling are the three main directions explored. Since redox enzymes are sizable proteins with anisotropic properties, achieving their functional immobilization requires a specific and controlled orientation on the electrode surface. All the factors influenced by this orientation are described, ranging from electronic conductivity to efficiency of substrate supply. The specificities of the enzymatic molecule, surface properties, and dipole moment, which in turn influence the orientation, are introduced. Various ways of ensuring functional immobilization through tuning of both the enzyme and the electrode surface are then described. Finally, the review deals with analytical techniques that have enabled characterization and quantification of successful achievement of the desired orientation. The rich contributions of electrochemistry, spectroscopy (especially infrared spectroscopy), modeling, and microscopy are featured, along with their limitations.

Keywords: metalloenzymes; enzyme immobilization; enzyme orientation; electrodes; bioelectrocatalysis

1. Introduction: Interest in and Limitation of Bioelectrocatalysis Based on Immobilized Redox Enzymes

1.1. Fundamental Issue: Understanding Energy Chains, and the Mechanism of Biocatalysis Involving Redox Enzymes

Electron Transfer (ET) is an essential process allowing a variety of microorganisms to find energy for growth. Depending on its environment, and especially on the available substrates, a given microorganism may find its energy through a combination of different metabolic pathways. A variety of redox proteins and enzymes are involved in those energy chains, displaying a variety of structural

motifs, cofactors, and metal content. Many of these individual proteins and enzymes can be identified, and fully characterized in vitro. The way they interact in vivo to fulfill the ET chain, however, often remains obscure. Furthermore, for a given metabolic pathway, some redox chains are favored for a given organism, and some proteins or enzymes may be over- or under-expressed. Depending on the environment or on the type of microorganism, one protein can replace another one as electron donor or acceptor for a specific process. Photosynthesis is one relevant example for which the involvement of one protein over another varies depending on the considered species (such as algae, cyanobacteria, or plants) [1]. Heme- (cytochrome c_6) or copper-containing proteins (plastocyanin), on the one hand, and FeS cluster- or flavin mononucleotide-containing proteins (flavodoxin), on the other hand, act as electron transfer shuttles allowing the coupling of water oxidation to $NADP^+$ reduction by photosystem I/photosystem II systems. Respiration of some exotic microorganisms known as extremophiles is also pertinent in this respect (Figure 1A). Although the latter are very interesting because they are sources of enzymes exhibiting outstanding properties, such as resistance to high temperatures, low pH, and high salinity, their electron pathways are far from being understood. In the respiratory chain of the acidophilic bacterium *Acidithiobacillus ferrooxidans*, two similar cupredoxins with close redox potentials are found, one soluble in the periplasm and the other anchored to the membrane. The reason for such redundancy in the electron pathway from ferrous oxidation to O_2 reduction is still unclear, despite many years of research on the organism [2]. Another relevant organism is *Aquifex aeolicus*, a hyperthermophilic ancestral bacterium which can sustain energy for growth from H_2 or H_2S oxidation coupled to either O_2 or sulfur reduction [3]. This feature leads to an intricate energy chain involving many enzymes interacting to sequentially transfer electrons within short timescales. Last, but not least, intramolecular ET also occurs inside an enzyme to transfer the electrons from the active site, where transformation of the substrate occurs, to the surface of the enzyme. In many cases, for huge enzymes in particular, the distance the electron must be transferred across is optimized by the maturation and incorporation of cofactors.

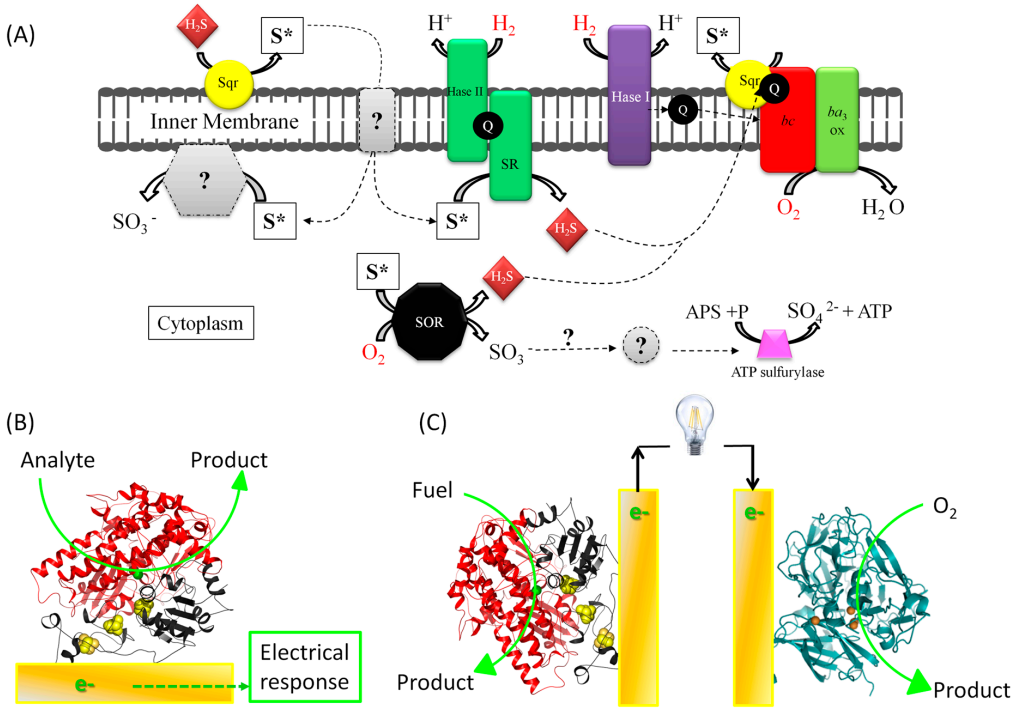

Figure 1. Electron transfer (ET) involving immobilized enzymes on interfaces: from metabolic ET chains (**A**) to biosensors (**B**) and enzymatic fuel cells (**C**). (**A**) is a schematic view of *A. aeolicus* metabolisms adapted from [3].

These few examples illustrate how the complexity of electron transfer pathways requires specific approaches to acquire some knowledge regarding the productive interaction between the involved enzymes and proteins. Common methods to analyze these fast ET processes include stop flow or chemical quench flow methods, as well as pulse radiolysis. Electrochemistry is another method of choice to quantify the rate of electron transfer processes. Not only can intramolecular ET within one protein be determined, but also the intermolecular ET between two interacting proteins can be characterized. The electron flow is then recorded as a current, which is related to the efficiency of the catalysis when an enzyme is involved. Furthermore, studying the ET between one protein and a conductive surface can mimic in vivo ET, because many of these processes occur at the surfaces of the interacting partners, or at the interface with the substrate. Interestingly, chemical functionalization of electrochemical interfaces has been a very active research field during the last years, since it provides a broad range of functionalities that will help to tune the interaction with a specific protein. Use of electrochemistry, however, requires as a first step the immobilization of the proteins or enzymes on conductive solid surfaces which act as electrodes, with the ultimate goal of keeping the protein structure as functional as possible.

1.2. The Applicative Issue: Use of Redox Enzymes Immobilized on Solid Conductive Supports for Biosensors, Bioreactors, and Biofuel Cells

Beyond fundamental knowledge of microorganism energy chains, the control and the functional immobilization of redox enzymes on conductive solid supports have found great interest in many environmentally friendly "green" biotechnological devices.

For these applications, the enzymes must be immobilized on the solid electrode surface in order to avoid diffusion into the biodevices, thereby losing the desired electrons, and compromising their effectiveness [4]. Among the currently developed biodevices, electrochemical biosensors have been the subject of extensive research for many years (Figure 1B). They have been preferred to other sensors such as those based on optical transduction because of the low cost and fast response of the electrochemical transduction. Large improvements in the detection limit down to fM concentrations, sensitivity, specificity, and stability of the biosensors have been achieved (see review [5] and references therein). This accomplishment is due to the identification and purification of new redox enzymes that are able to act as a recognition element, combined with the development of new conductive matrices for their efficient immobilization, essentially on the basis of large-surface-area nanomaterials. Electrochemical biosensors are used in many different domains, among which medical applications [5], food safety, and environmental monitoring [6] are those undergoing the largest developments. The earliest electrochemical biosensor for biomedical applications dates back to 1962, and uses the redox enzyme glucose oxidase to measure sugar in blood [7]. The increasing knowledge of the parameters that control enzymatic activity on electrodes has enabled the design of the current commercially available «finger-pricking» approach, and has opened the way to implantable glucose biosensors. Advanced technology allows us to now envision the integration of the glucose bioelectrochemical sensor in a smartphone platform, simplifying the lives of diabetic patients [8]. Furthermore, it is possible to measure glucose in other fluids than blood, i.e., interstitial liquid, urine, saliva, sweat, or ocular fluid [9]. These last developments have led to the design of new robust enzyme-decorated bioelectrodes, such as flexible electrodes [10]. Many other targets are detectable by electrochemical enzyme-based biosensors, such as nitric oxide [11], cholesterol [12], urea [13], or influenza virus [14]. In the domain of the environment, bioremediation is a process that involves redox enzymes for cleanup [15]. Oxygenases and multicopper oxidases (MCOs) are, for example, very efficient in the degradation of chlorinated and phenolic compounds. In this case, it should be productive to immobilize the enzyme on a conductive support to promote bioremediation by use of electrochemical methods.

More recent applications in the domain of bioreactors for fine chemistry have found great interest in the original use of redox enzymes immobilized on conductive supports. The two following examples illustrate this increasing research field nicely. A mandatory step for wide use of enzymes in biocatalysis

is the regeneration of nicotinamide adenine dinucleotide phosphate, known under its redox couple $NADP^+$/NADPH. Actually, this cofactor is required for the function of a large number of identified enzymes that are efficient in industrial processes such as the production of alcohols, hydroxylation of aromatic compounds, hydrolysis of triglycerides, or Baeyer–Villiger reactions [16]. Economic considerations impose the regeneration of NADPH, as it is costly to synthesize it. Among the methods explored for that purpose, electrochemical ones would be of great interest thanks to their low cost and simplicity. In this case, the activity of enzymes immobilized on various electrodes would be one attractive way to regenerate the cofactor. The second example is the electrochemical reduction of CO_2 into fuel products, with the additional advantage of providing a method for CO_2 sequestration. Biology offers natural biocatalysts able to achieve CO_2 reduction with high efficacy. Although the current research mostly focuses on whole microorganisms colonizing electrodes [17], encouraging results have been reported on the activity of specific enzymes [18]. Here, the mandatory step would again be the functional immobilization of the enzyme on the electrode surface.

Finally, one emerging domain where the immobilization of redox enzymes is mandatory is the sustainable production of electricity. Fuel cells can be considered as green devices for electricity generation, since they produce no greenhouse gases. However, the transformation of H_2 and O_2 at the anode and cathode of the fuel cell requires catalysts based on expensive noble metals such as platinum. Some redox enzymes are known to catalyze fuel oxidation and oxidant reduction with high efficiency and specificity. This possibility opens the route for the development of the so-called enzymatic fuel cells, where the catalysts are the redox enzymes (Figure 1C). Two main categories of biofuel cells exist, mainly depending on the intended application and on the fuel used, with the oxidant being, in most cases, oxygen. The proof of concept of the first biofuel cell category appeared more than 40 years ago. It is based on the oxidation of glucose by flavin-based glucose oxidase or cellulose dehydrogenase. Many applications are targeted. As an illustration, one can cite biobatteries, small enough to be implanted in blood for feeding medical devices, such as a glucose biosensor or an insulin delivering pump, biobatteries implanted on ocular lenses to monitor ocular pressure, or biobatteries stuck on the skin to monitor lactate in sweat. Recent reviews report the major current developments in that type of biofuel cells [19]. A more recent concept uses the same fuel as in platinum-based fuel cells, with the aim of enhanced power output compared with sugar/O_2 enzymatic fuel cells. Here, hydrogen oxidation is carried out by the highly efficient hydrogenases, whose active site is composed of nickel and iron atoms. Coupled to MCOs for oxygen reduction, H_2/O_2 biofuel cells display an open circuit voltage of around 1.1 V, depending on the origin of the enzymes, which is the highest ever reported for biofuel cells [20]. Late development of this new biofuel cell generation relies on the hydrogenases themselves, which—intrinsically—are very sensitive to oxygen. This sensitivity was observed for most of the enzymes known before the identification of some extremophilic hydrogenases from microorganisms able to sustain energy from a hydrogen–oxygen metabolism. These latter hydrogenases were demonstrated to be oxygen-tolerant and, moreover, resistant to carbon monoxide, opening the way to their use as biocatalysts in fuel cells. This second category of biofuel cells could be employed to power environmental sensors, with an additional advantage over platinum-based fuel cells. Indeed, thanks to the specificity and properties of some hydrogenases, it becomes possible to use nonpure H_2, as hydrogen produced from biomass or waste. Recent research shows that high current densities in the order of 10 mA/cm^2, and all the most high currents reported (up to 1 A per mg of enzyme) can be reached, which is very promising [21].

1.3. Limitations of Bioelectrocatalysis: Stability, Wiring, and Interrelationships

For both fundamental research and applied perspectives described earlier, the main first step is the productive immobilization of redox enzymes on electrochemical interfaces. The aim is to optimize the ET rates both for intermolecular and interfacial ET, in order to ultimately optimize bioelectrocatalysis efficiency. Concomitantly, stabilization of the enzymes once immobilized would be desired. Many recent reviews analyze the issues relative to protein behavior once immobilized on solid

supports [22]. Although no general rules can be formulated, it is plausible to expect that the interaction between the solid support and the enzyme may cause an alteration in protein structure and/or flexibility, hence modifying its properties. Depending on the enzyme and on the support, enhanced stability and activity, or, on the contrary, destabilization may be observed. Immobilization may prevent enzyme aggregation, thus enhancing catalysis when compared with free enzymes in solution. Proper immobilization on a solid support mimicking the enzyme native environment may improve enzyme activity. Here, we particularly want to highlight the specific aspects of trying to perform conductive electron transfer processes by using a conductive surface for enzyme immobilization. With this goal in mind, additional principles have to be taken into account, and some of the general rules admitted for an efficient and stable immobilization process no longer hold. As an example, it is expected that in order to achieve high catalysis efficiency, nonredox enzymes must be oriented with the active site turning to the opposite side of the solid surface to facilitate substrate access. In the case of ET however, the situation is the opposite, since the ET rate strongly depends on the distance between the electrode and the active site. Hence, an orientation of the enzyme with the active site as close as possible to the solid surface will be targeted. This situation will be discussed further in the following. Along the same lines, it is also admitted that deleterious interactions between an enzyme and a surface should be avoided by introducing a linker on the enzyme. In the case of ET, however, this linker introduces an additional distance that can be prejudicial to the ET efficiency. Furthermore, the enzymes on conductive supports will be subjected to electric fields, as soon as the bioelectrode is polarized at the required operational potential. This operational condition implies that redox enzymes on solid electrodes must not only resist various nonphysiological environments (salt concentration, nonbuffered solution, etc.) but also resist high current flow, or a wide range of redox potentials.

These general considerations clearly illustrate that redox enzyme immobilization on solid electrochemical interfaces raises issues that are different from the general issues of enzyme immobilization on solid supports. The goal of the present review is to describe these specific aspects, and it will focus on the main parameters that govern the functional immobilization of redox enzymes on electrodes, as well as the current tools available to rationalize and control these parameters. We will limit our discussion to planar electrodes, for which fundamental studies of immobilized redox enzymes are more relevant, as discussed hereafter.

2. Interfacial Electron Transfer: Why Is Orientation a Key Issue?

The maturation of the idea to use redox enzymes in biodevices was driven in parallel by the increasing understanding of the ET mechanism in the context of biological processes [23]. According to Marcus theory, the ET rate k_{ET} between an electron acceptor and an electron donor is a function of the potential difference between the electron acceptor and donor, given as the Gibbs free energy of activation (ΔG), and of the reorganization energy [24]. k_{ET} can be expressed as $k_{ET} = \alpha(r)\upsilon\, e^{-\Delta G/RT}$, where $\alpha\upsilon$ depends on the electronic coupling between the reactants, with the transmission coefficient α exponentially varying with the distance r separating the donor and the acceptor. Based on this theory, the maximum distance of electron tunneling between donor and acceptor was estimated to be 20 Å [23,25]. Actually, this is the distance which is reached through complex formation between the active sites of two interacting proteins. The upper distance limit of 20 Å is also observed in many enzymes for the separation of active sites and electronic relays, although electrons can travel longer distances through conserved aromatic residues of the protein moiety [26]. As a consequence, the intramolecular ET does not limit the catalysis since k_{ET} is much higher than catalytic constants [27]. Considering now the electrode as the donor or the acceptor, the rule can be extended to define the limiting distance separating it from the enzyme for ET. As enzyme diameters are on the order of a few nm, active sites are often more distant from the surface than the predicted maximal distance for fast ET within the electrode. The consequence is that for interfacial ET to proceed, it is mandatory to place the active site at a distance compatible with ET, using controlled tethering to the surface. Because the active site is often protected from the external environment by deep embedding inside the protein

moiety, one has to play with the electronic relays inside the enzyme which allow fast intramolecular ET. The electron entry or exit point will be the particular electronic relay on the surface of the enzyme that must be located at a close distance from the electrode (Figure 2). The molecular-level features favoring a specific orientation can be determined based on the examination of the crystallographic structure of the enzyme, possibly in combination with molecular modeling approaches [28]. Nevertheless, it is experimentally very difficult to succeed in a single-point attachment of an enzyme on an electrode surface. The immobilization of the protein will often lead to a distribution of enzyme orientations. Even in the case of enzyme immobilization through specific anchors grafted on the enzymes (this will be discussed below), one cannot exclude ET through a variety of pathways because of enzyme flexibility on the surface. As the interfacial electron transfer constant k_0 between the enzyme and the electrode surface depends on the distance of the electron tunneling, the distribution in the enzyme orientations creates a dispersion of this constant that may lie in the range between k_{min} and $k_{max} = k_0$. In the case of ahomogeneous distribution of enzyme orientations we have $k_{min} = k_0 \exp(-\beta d_0)$, where βd_0 is a parameter that represents the dispersion of possible orientations the enzyme molecules may adopt while maintaining electron exchange with the electrode. The βd_0 parameter governs the shape of the electrochemical signals as modeled by Armstrong's group [29], and reported in recent papers for the analysis of the ET of immobilized enzymes [30].

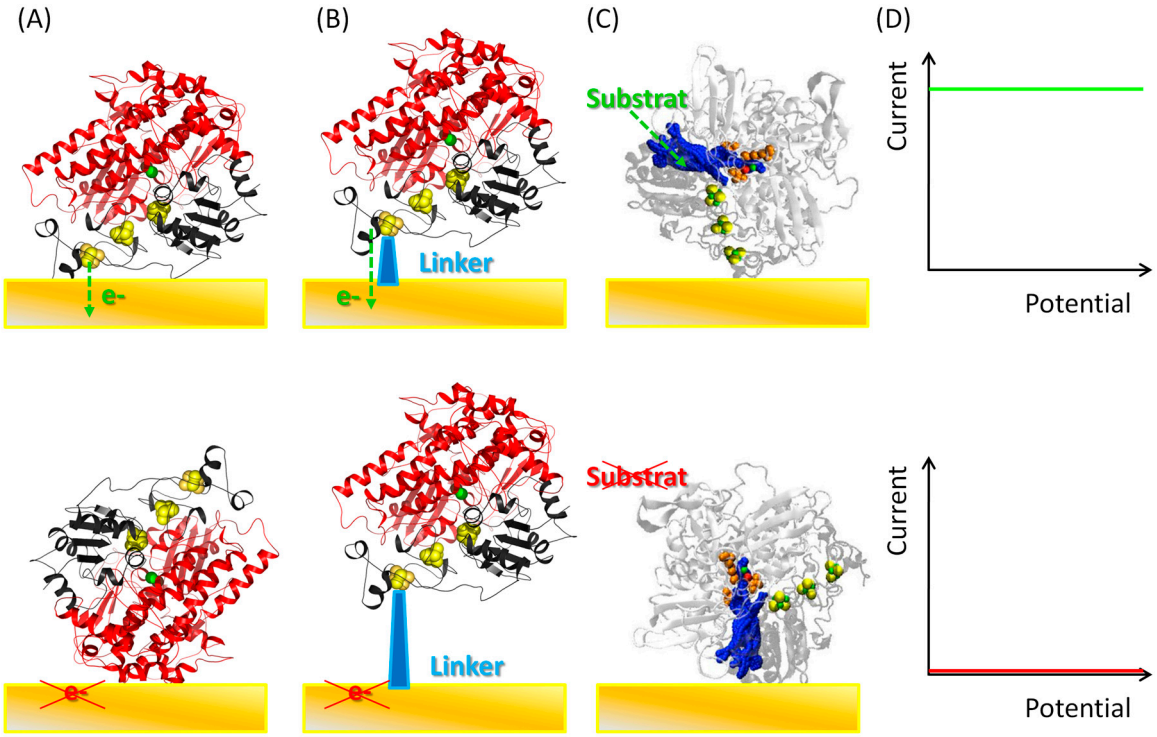

Figure 2. Schemes of enzyme immobilization conditions (**A**–**C**) allowing or precluding a direct electrical connection (DET) (**D**) at an electrochemical interface. (**A**) Illustrates how the distance between the active site, or a surface electronic relay, of an adsorbed enzyme and the electrode influences DET; (**B**) Illustrates the effect of the length of a linker used for enzyme immobilization on DET; (**C**) Illustrates the effect of the substrate channel access upon enzyme immobilization on DET.

Note that the enzyme orientation on the electrode is not only a key issue for interfacial electron transfer, but is also essential to facilitate the diffusion of substrates and products within the enzyme internal cavity network toward the catalytic site. Molecular Dynamics simulations on [NiFe] hydrogenases from *A. aeolicus* and *Desulfovibrio fructosovorans* have shown how these two homologous enzymes display their own specific internal tunnel network [31]. In the case of the

membrane-bound *A. aeolicus* hydrogenase, all the substrate entry points are located on the same side of the enzyme's surface. As a consequence, the enzyme's adsorption on an electrode with the wrong orientation might result in the shielding of some parts of its surface, such that a small substrate could no longer use it as an entry point to reach the active site.

3. The Key Components

3.1. Properties of Redox Proteins

Enzymes are large biomolecules that are abundantly found in living organisms with great variety and very specific functions. As biocatalysts, enzymes accelerate reactions by decreasing their activation energy. They are composed of one or more long chains of amino acid residues displaying a vast array of functions within organisms, including catalyzing metabolic reactions, DNA replication, and responding to stimuli. The structure of such proteins stands out as complex but with a high degree of organization compared to small molecules, as required to fulfill high selectivity. This structure/function relationship will have strong impact on further functional enzyme immobilization. Tertiary structures form by folding of the α-helix and pleating of the ß-sheet in such a way as to achieve maximum stability or the lowest energy state. The final shape of the protein is stabilized by various interactions, including hydrogen bonding, disulfide bonds, ionic bonds, Van der Waals, and hydrophobic interactions. Coarse-grain modeling approaches can provide useful insight on the thermal unfolding of surface-immobilized enzymes [32]. More generally, how the immobilization will alter this structure is, of course, of great importance.

Among enzymes, redox enzymes are those proteins whose established role is to convert a substrate along an energy chain through electron exchange. They consist of a redox center, required for their bioactivity, with the ability to either accept or donate electrons. Different types of redox centers can be found in redox enzymes, ranging from metal-based ones (Ni, Fe, Mo, Cu, etc. . . .) to inorganic ones such as flavin adenine dinucleotide (FAD), acting as a cofactor. In metalloenzymes, the metal ion is usually held by coordinate-covalent bonds on the amino acid side chains or inorganic ligands, or is bound to a prosthetic group (e.g., heme). The redox active center is very often embedded in the polypeptide structure, which protects it against hostile environments but, from a conductive point of view, insulates it. Different strategies have been used during maturation to succeed in a fast intramolecular ET, which is not limiting compared with the catalytic efficiency; this is illustrated hereafter by some relevant examples, widely studied in the literature (Figure 3).

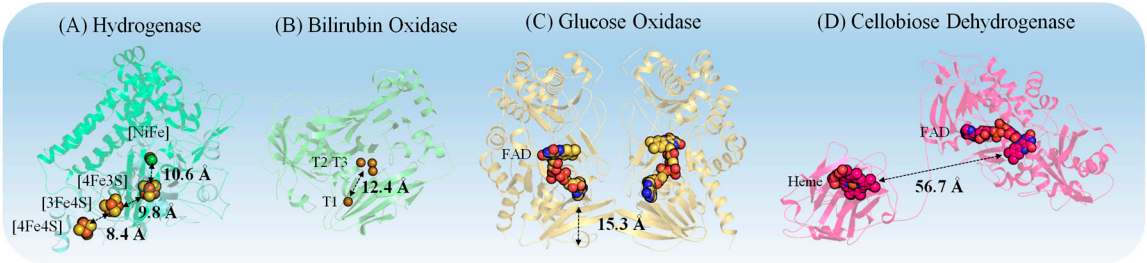

Figure 3. Representation of relevant distances for intramolecular and interfacial ET in several redox enzymes: metal center to metal center, metal center to cofactor, or cofactor to protein surface. (**A**) *A. aeolicus* hydrogenase model [31]; (**B**) Bilirubin oxidase (pdb ID: 2XLL); (**C**) Glucose oxidase (pdb ID: 1CF3); (**D**) Cellobiose dehydrogenase (pdb ID: 4QI7).

MCOs [33] such as laccases (LAC), bilirubin oxidases (BOD), or cuprous oxidase (CueO) are copper-containing enzymes that efficiently catalyze oxygen (O_2) reduction directly to water [34]. BODs and LACs are found in fungi, plants, and bacteria, where they catalyze the oxidation of bilirubin to biliverdin and the oxidation of polyphenol compounds, respectively. O_2 reduction requires four

copper sites which differ by their ligand coordination and geometry: one T1 Cu, and a trinuclear cluster composed of one T2 Cu center coupled to a binuclear T3 Cu center [34]. Physiologically, electrons are received from the substrate to the T1 Cu, and are transferred through a histidine–cysteine bridge to the trinuclear cluster 12–14 Å away, where O_2 reduction takes place [35]. In a mimicking way, one can imagine how an electrode can provide the electrons instead of the physiological substrate, which means that the electrode has to be wired to the copper T1.

Hydrogenases (Hases) are the enzymes that catalyze the reversible oxidation of molecular hydrogen (H_2) and reduction of protons. They are found in the periplasm or cytoplasm of various microorganisms, in many different environments, where their main role is to provide energy for the organisms by oxidation of molecular hydrogen. Hases are subclassified into three different types based on the active site metal content: iron–iron Hases, nickel–iron Hases, and iron Hases [36]. The [FeFe]-Hases are more specifically involved in H_2 production from proton reduction, whereas [NiFe]-Hases are more efficient in H_2 oxidation [37]. In the latter case, the [NiFe] active site, where the hydrogen binds, is buried deep inside the large subunit. To transfer the electrons from/to the active site, 3 FeS clusters less than 13 Å distant from each other constitute a conductive line in the small subunit towards/from the surface of the enzyme. Hydrogen reaches the active site through well-defined hydrophobic channels, [38] whereas avenues for proton evacuation are not yet so clearly identified. If one wants to immobilize such an enzyme, two conditions need to be met: (i) wire the enzyme to the electrode via the FeS cluster located closest to the surface of the protein; and (ii) make sure the channels for the substrate access and products removal are accessible.

Glucose oxidase (Gox) is the most studied redox enzyme so far, and catalyzes the oxidation of β-D-glucose to D-glucono-1,5-lactone and hydrogen peroxide using molecular oxygen. It is a large dimeric protein with a molecular weight of 160 kDa and an average diameter of 8 nm, containing one tightly bound FAD per monomer as a cofactor [39]. The FAD cofactor is deeply embedded inside the protein matrix. In addition, it was experimentally shown that the FAD molecule is located in a cavity deeper than 8 Å [40]. Various attempts have been made to establish the wiring between the active center of GOx and various electrodes [41]. However, many discrepancies in the results are reported, and uncertainty remains regarding the retention of the conformation of the enzymes.

Cellobiose dehydrogenases catalyze the oxidation of various saccharides into lactones. Their strategy to transfer electrons is different from Gox as each monomer consists in two domains, one with a FAD cofactor and the other with a heme. ET proceeds physiologically from the substrate to the FAD cofactor and finally to the heme. The latter is accessible to the solvent, and is connected to the FAD domain through a flexible linker [42], which can be a great advantage if using this type of enzyme on an electrode surface.

These few examples clearly indicate that the strategy required to succeed in the ET from/to the enzyme to/from the electrochemical interface will largely depend on the structure and specific features of the enzyme. Apart from fast intramolecular ET achieved thanks to electronics relays within the enzyme, ET between physiological partners in a given chain, or between the substrate and the enzyme, is facilitated by specific recognition surfaces involving both hydrophobic and hydrophilic moieties [43]. As illustrations, the third, surface-exposed FeS cluster in the [NiFe]-Hases from *Desulfovibrio* is surrounded by an acidic patch composed of glutamic amino acid residues, which recognize a lysine-rich environment of the interacting heme of the physiological partner, a cytochrome c_3 [31,44]. This electrostatic interaction allows both partners to come to a close distance which then induces fast intermolecular ET. Various other striking examples of electrostatic-driven protein–protein interactions for efficient ET are documented in the literature: interaction between cytochrome *c* oxidase and cytochrome *c* [45], sulfite reductase and ferredoxin [46], cytochrome P450 and putidaredoxin [47], and NADH-cytochrome b_5 reductase and Fe(III)-cytochrome b_5 [48]. Also, the Cu T1 in LACs is inserted in a hydrophobic pocket which allows favorable interaction with its natural organic substrates [49]. The knowledge of such recognition interfaces will become a key issue once a rational approach to immobilize enzymes on electrodes is envisioned.

Furthermore, from the 3D structure of given redox enzymes, it is possible to calculate the surface electrostatic potential distribution which indicates the existence of dipole moments [50]. A dipole moment, in the simplest case, is a vector quantity representing the separation of two opposite electrical charges. The magnitude of this quantity is equal to the distance between the charges multiplied by the charge. The direction of the vector is from negative to positive charge. In the general case, the dipole moment can be computed by the formula $\vec{\mu} = \sum_i q_i \times \vec{r_i}$, with $\vec{\mu}$ as the overall dipole moment generated by i charges, q_i as the magnitude of each partial charge i, and r_i as the position vector of charge i. Such calculations provide an initial understanding for preferential orientations of immobilized enzymes on electrodes, a feature that may be exploited to favor high ET rates. Another key aspect of enzymes is their internal cavity network that enables the diffusion of substrates/reaction products between the solvent and the enzyme's catalytic site, and which can also be investigated via modeling and free energy calculation [51]. From a theoretical perspective, the ET itself can be simulated using a wealth of different techniques involving mixed Quantum–Classical molecular dynamics (MD) simulations, Quantum Mechanics/Molecular Mechanics (QM/MM) approaches, or numerous Density Functional Theory (DFT) variants [52].

3.2. Conductive Electrode Surfaces

A large variety of electrodes are available, displaying high electric conductivity and mechanical and thermal stability. During the last years, a great deal of research has focused on the immobilization of redox enzymes in and on 3D conductive materials. The idea underlying the use of high surface area/volume materials is to enhance the loading of redox enzymes and, hence, the current for biocatalysis. Carbon-based materials such as carbon nanotubes, carbon nanofibers, carbon felt, or metal nanoparticles have been demonstrated to act as a very efficient host matrix [53]. It is also expected that tuning the size of the pores of the matrix may help in the stabilization of the enzyme by multipoint anchoring [54]. The control of enzyme loading and specific activity in such large-area materials is, however, in most cases hampered by the lack of methods able to monitor one individual enzyme in the matrix. In addition, homogeneous distribution and orientation of enzymes in the 3D network is rarely achieved. Nonetheless, it is worth mentioning the original work of Vincent's group, who set up a Protein Film Infrared Electrochemistry (PFIRE) method for the monitoring of the enzyme conformation entrapped in carbon black particles [55]. Mazurenko et al. also reported the resolution of enzyme partitions in carbon felts [21]. Nevertheless, it appears more relevant to study the immobilization of redox enzymes on more planar electrodes, to achieve easier control of the enzyme conformation, and to overcome mass transport and substrate partition issues arising from the surface meso- or nanoporosity which induces local variation of substrates and products (such as local acidification, for example) and complexifies the whole process. The notion of planarity itself must be discussed here. Given an average size of enzymes in few nanometer ranges, all materials that present macroporosity should be considered as planar from the enzyme immobilization point of view. However, macroporosity is most often accompanied by mesoporosity, in which the enzyme is connected through many points. Any porous materials should thus be considered as nonplanar.

Smooth metal surfaces like Au, Ag, and Pt, or more complex surfaces such as indium–tin–oxide (ITO), or flat carbon-based surfaces such as glassy carbon can be used for the immobilization of redox enzymes, as well. However, even these surfaces considered as planar present a roughness factor that may influence enzyme immobilization. Few studies report the effect of roughness on bioelectrocatalysis. It is worth noting the work from Thorum et al. in which roughness was induced on a gold electrode to force protruding of functionalities required to get access to the enzyme active site [56]. Gold supports/electrodes of different geometries are commercially available and are the model supports for analytic and surface-addressing techniques like Surface Plasmon Resonance (SPR), Quartz Crystal Microbalance (QCM), Polarization Modulation Infrared Reflectance Absorption Spectroscopy (PMIRRAS), Surface-Enhanced Infrared Absorption (SEIRA), and ellipsometry. As the chip used in these methods can also serve as the electrode for electrochemical sensing, the gold

surface appears all the more relevant when dealing with redox enzyme immobilization. In principle, single-crystal/monocrystalline gold surfaces should be used in all these techniques because they provide a controlled gold surface at the atomic level. However, the reusability of the surface is critical, whereas improved understanding of surface pretreatment for polycrystalline gold allows preparing reproducible surfaces [57]. Hence, polycrystalline gold surfaces, where the distribution of metal atoms is nonuniform throughout the electrode surface, are very handy. Surface treatment provides surface control and promotes their wide use for protein electrochemistry [58]. Electrochemical cleaning by cycling in H_2SO_4 solution between −0.35 V and +1.5 V vs. Ag/AgCl allows calculating of the real electroactive surface area by integrating the gold oxide reduction peak at +0.9 V, taking into account a charge of 390 $\mu C \cdot cm^{-2}$ for the reduction of a gold oxide monolayer [59]. The roughness factor can thus be calculated ($R_f = A_{electroactive}/A_{geometric}$), which represents the difference between the projected geometric surface area and the electro-accessible surface area. R_f takes values around 2 to 5 depending on the kind of surface considered and the cleaning procedure [60].

Several spectroscopic methods have been coupled to electrochemistry taking advantage of conductive biocompatible materials. Surface-enhanced vibrational spectroscopies benefit from nanostructuration of the metal (Au or Ag) to increase their sensitivity (enhancement factor in absorption: 10^2–10^6) [61]. Because of the nanostructuration surface, here also a roughness factor can be calculated ($R_f = A_{real}/A_{geometric}$); the geometric area ($A_{geometric}$) represents a flat surface while the real area (A_{real}) is experimentally accessible, for example, via electrochemistry or AFM [60,62,63]. On the other hand, infrared spectroscopy based on reflection absorption techniques requires flat reflective surfaces [64]. While monocrystalline gold remains the most commonly used support, it was recently shown that despite lower-intensity infrared signals, glassy carbon is a promising alternative for broadening the applications related to electrochemistry [65].

A molecular-level picture of these surfaces can be obtained through modeling approaches such as MD simulations. Interestingly, the last decade has seen the development of numerous force fields (FF), specifically parameterized to model a large variety of solid surfaces [28]. Amongst the material models that are now accessible to computational chemists, one can mention metallic surfaces (Ag, Al, Au, Cu, Ni, Pb, Pd, Pt), for which Lennard-Jones potentials for nonbonded interactions have been developed [66]. Gold in particular can be modeled in common simulation codes such as GROMACS and NAMD using either the GolP atomistic force field [67] or the METAL/INTERFACE force field [68]. Additional materials of interest for bioelectrochemistry can be modeled such as silica [69], but also graphite [70] or carbon nanotubes [71]. These latter materials cannot be considered as planar surfaces, however. An important issue when studying the adsorption of biomolecules with considerable dipole moments, such as redox enzymes, is the surface polarization, which can contribute to up to 20% of the total binding energy between the protein and the surface [72]. This aspect is taken into account in the GolP-CHARMM FF for gold surfaces [73]. Another FF that incorporates polarization is the AMOEBA FF [74], which was already extended to model peptides on a graphene surface [75]. Still, development efforts in that field are mostly directed towards solvated biomolecules, and a lot remains to be done for the simulation of interfaces.

3.3. Interaction between Enzyme and Conductive Surface: How Can It Be Modulated?

Enzymes can be immobilized on the electrode surfaces following different processes including simple adsorption, entrapment in a complex matrix such as redox polymers, and covalent binding [76,77]. Among the challenges of immobilizing enzymes onto electrodes, preserving the native conformation and catalytic properties, and providing good electrical connection and relative stability are of outmost importance. In this respect, one philosophy of immobilizing enzymes is based on considering the electrode as a surrogate to the known physiological partner of the enzyme: a substrate, a cofactor, heme- or [Fe-S]-based protein shuttles, etc. To get a proper enzyme immobilization for the optimum ET, mimicking physiological interactions between partners, it is thus of great importance to gain the possibility to tune the interactions between enzymes and the electrode surface.

Two main options exist when trying to tune the interactions between a redox enzyme and an electrode: (i) chemical functionalization of the electrode surface; and (ii) engineering the enzyme.

3.3.1. Electrode Functionalization

Several methods have been developed to add surface chemical functions to planar electrodes [78] (Figure 4). Concerning gold surfaces, the most widely used functionalization is achieved through self-assembled monolayers (SAMs). SAMs are usually formed by spontaneous adsorption of sulfur. Alkanethiols, or dialkyl disulfides or sulfides possess high affinity for the surface of gold (but also for platinum or silver), with a bond energy of RS-Au of ~40 kcal·mol^{-1} [79]. This adsorption results in well-defined organic surfaces with desirable and alterable chemical functionalities, controlled simply by changing the terminal group of the thiol chain. The modification of a gold electrode with SAMs provides a choice of positive/negative/hydrophobic terminal functional groups such as –COOH, –NH_2, –SO_3H, –CH_3, and –OH. In addition, the knowledge of the pKa of the terminal moieties allows chemical control on the electrode surface. As examples, pKa values of 6.0 [80] and 6.9 [81] for SAMs of 11-mercaptoundecanoic acid (MUA) and 4-aminothiophenol (4ATP) groups on gold were determined, respectively. Dependence of the pKa of –NH_2-based SAMs on thiol chain length was also reported [82].

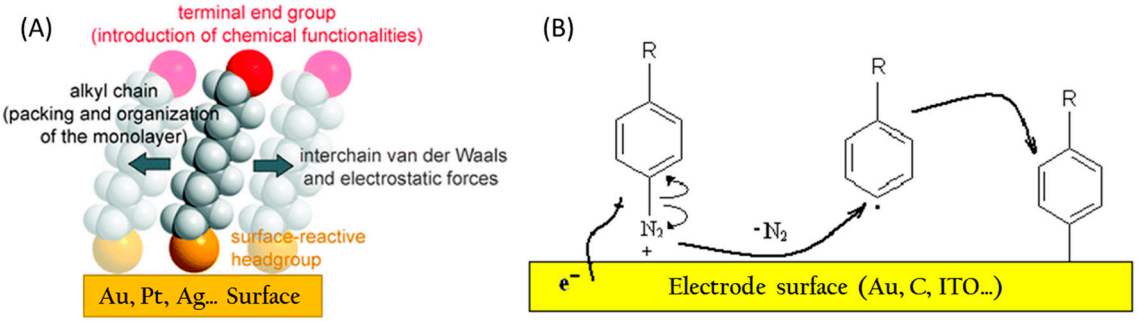

Figure 4. Representation of (**A**) self-assembled monolayer [83] and (**B**) scheme for electrografting of diazonium salts on electrode surfaces (Au, C or Indium Tin Oxide (ITO)) with alterable terminal chemical functionality.

Their ease of preparation from millimolar thiol solutions makes SAMs attractive candidates for surface tailoring. A surface coverage of the order of pmol·cm^{-2} is generally achieved and adsorption stops at the level of monolayer coverage [84]. This surface coverage, as well as compactness and organization of the layer, shows, however, dependence on the type of thiol molecules, nature of the metal surface, immobilization time, and thiol concentration [85]. Longer adsorption time and longer thiol chains are expected to provide a more organized SAM layer by decreasing pinhole defects or conformational defects in the alkane chains [86,87]. Long-chain thiols are expected to form well-organized assemblies due to stabilizing van der Waals interaction along the adsorbed chain. On the contrary, presence of long chains may screen their mobility in the solution and, hence, their accessibility to the metal surface. It was recently proposed that fast and repeated changes on applied potential pulses relative to potential of zero charge cause an ion stirring effect [88] which has an influence on the SAM formation kinetics. Immobilization of biomolecules on SAMs has been critically reviewed [89]. The possibility to prepare mixed SAMs is an added advantage, where homogeneous or separated phases of different thiols may allow the site-specific binding of enzyme to the surface [90].

Besides this, silane-based SAMs on ITO electrodes have been used owing to their simple preparation, good reproducibility, and high stability [91]. ITO, being low cost, highly stable, and transparent, is a very useful material as an electrode due to its electrical and optical properties [92] and plays an important role especially for biosensor technology [93]. The silane-based chemicals act as

cross-linkers because they contain Si–O bonds which react with the surface hydroxyl groups of ITO where the end groups of silane act as an immobilization matrix for biomolecules.

However, the use of SAMs for redox enzyme immobilization also raises critical issues. The first is linked to the ET process through the SAM itself, which can become a limiting step and control the whole ET process. As developed above, the efficiency of ET, given by the ET rate constant k_{ET}, is found to be a function of the distance d between the electrode surface and the redox species. A study related to the kinetics of ET between a gold electrode and a SAM of thiol of variable length confirms the exponential dependence of the rate constant on the chain length [94], according to $k_{ET} = k^{\circ} \exp[-\beta d]$. In the case of SAMs, an additional parameter is the surface coverage, θ, after SAM formation. For a complete monolayer of SAM without any defects (θ = 1), the mechanism of ET is tunneling, as the monolayer shows blocking behavior. Therefore, the expression for the ET rate constant can be read as $k_{tunnel} = k^{\circ} \exp[-\beta d]$, where k° is the rate constant for a bare electrode, β is the constant of electron transfer through tunneling, and d the thickness of the SAM. This is the case for chemisorption of long-chain thiols on a gold surface, which usually results in well-organized monolayers with minor defects due to effective van der Waals interactions along the carbon chains [95]. Another mechanism is based on a membrane-like behavior of the SAM, so that redox species can permeate through the monolayer, and ET to/from the electrode takes place. This kinetic process is controlled by the partition coefficient, κ, between the solution and the membrane, the diffusion coefficient, D_f, in the membrane, and the kinetics of material transport at the film/solution interface with a rate constant, $k_{interface}$ [96]. In the presence of pinhole defects within the SAM, another ET pathway may be effective due to diffusion of the redox species through the defect sites to the electrode. This alternative transfer may operate in the case of short thiol chains which are expected to display less organized layers. All these ET phenomena may take place in parallel and an effective rate constant will reflect the relative contributions of the different pathways [97] (Figure 5). As an implication, for ET to proceed, a balance is needed between a sufficiently high ET rate and sufficient organization to be able to obtain a controlled SAM. This can be reasonably achieved by maintaining the length of thiols comprising around 6–8 carbons [98].

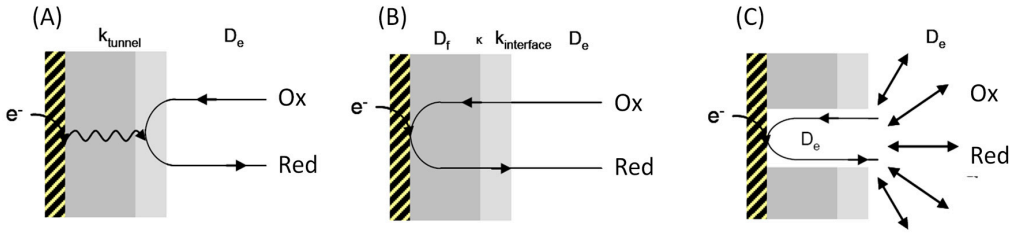

Figure 5. ET processes through a self-assembled monolayer (SAM) (in grey) formed on an electrode. (**A**) Tunneling ET process through a compact SAM; (**B**) ET through a SAM behaving as a membrane. ET will be controlled by a partition coefficient at the membrane/solution interface and by the diffusion coefficient inside the membrane; (**C**) ET proceeds through defects in the SAM. D_e and D_f are the diffusion coefficients in the electrolyte and in the SAM, respectively. Ox and Red designate a redox couple in solution. Adapted from [96].

The second critical issue is linked to the poor stability of the SAM, especially when the potential of the electrode is polarized to extreme values of potentials [99]. The Au–S bond is found to be stable only in a small potential window i.e., −0.6 to +0.6 V vs. Ag/AgCl [100]. Thiol-based SAMs are also sensitive to heating, and their thermal stability is limited to 400 K [101]. Above this temperature, thiol molecules start to desorb in the form of disulfides, suggesting that the Au–S bond is weaker than the S–C bond of thiols [102]. Some discrepancy, however, exists about the thermal stability of monolayers of thiol [103]. SAMs formed by long-chain thiols appear to be more thermally stable due to their well-organized nature on the surface [104].

As a consequence of the poor stability of the Au–S bond, a carbon–gold (Au–C) bond should be preferred [105]. Reduction of aryl-based diazonium salts is a widely used method to prepare functionalized surfaces, not only on carbon, but also on gold electrodes [106–108]. The interest in such modifications concerns the wide range of functional groups available that are associated to high stability over a large potential window. Formation of mixed monolayers by successive electrochemical reductions from a mixture of diazonium salts presents an added advantage towards surface functionalization [109,110]. The disadvantage is the difficulty to stop the reaction at the monolayer formation. Electrografting of aryl compounds on electrode surfaces is based on the formation and attachment of highly reactive aryl radicals. However, polymerization between two aryl radicals, and their chemical reaction with already adsorbed aryl molecules may compromise the quality of the monolayer. Possible control of the monolayer can be achieved by utilizing a so-called "protecting–deprotecting" approach, where a bulky group protects the functional group, avoiding both the formation of disordered multilayers and possible reaction of functional end groups with aryl radicals. Organization of the monolayer is typically controlled by the size of the protecting group [111]. On the other hand, the chemical substituent groups attached to the benzene ring of diazonium salt can significantly affect the electrografting of these molecules on the electrode surface, first due to their size and second due to their nucleophilic/electrophilic nature. QCM measurement was used to probe the thickness of the electrodeposited aryl organic layer on an Au electrode, and suggested that the large size of the substituent and its steric hindrance typically led to the formation of thin layers [112]. A recent study related to the kinetics of electrografting on gold surfaces also suggested that the presence of an electron-attracting group increases the rate of reaction of the aryl radical on the gold surface [113], whereas the presence of an electron-donating group slows down the grafting process, thereby offering control over the possibility to form monolayers. It should be noted that a mixed layer of aromatic diazonium salt and thiol can be advantageously used, as demonstrated in the case of LAC on gold electrodes. A submonolayer of aryl groups was formed to minimize multilayer formation by aryl radical attack, while full electrode coverage was achieved by further thiol adsorption [114].

Other tools to functionalize planar electrodes are noteworthy. Among additional immobilization strategies, a variety of amines can be covalently attached to the electrode surface through their electrooxidation onto the electrode [115]. Immobilization via in vivo natural enzyme substrate can be used alternatively to significantly increase electrocatalytic activity relative to simple protein adsorption on the electrode. Bilirubin is the natural substrate for BODs, which is in vivo oxidized to biliverdin with the reduction of oxygen to water. BOD was immobilized on a pyrolytic graphite (PG) electrode prefunctionalized by bilirubin, and a twofold increase in electrocatalytic activity in terms of current was reported compared to a bare PG electrode [116].

Infrared spectroscopy is a perfect tool to monitor an electrode functionalization and to judge the quality of the immobilization procedure regarding its impact on the protein structure. IR spectroelectrochemistry allows simultaneous monitoring of electrochemical signals and infrared spectra reflecting the secondary structure of the enzyme (Amide I and Amide II bands centered at ~1650 cm^{-1} and ~1550 cm^{-1}, respectively). However, one important aspect when choosing an immobilization procedure is to avoid spectral interference between the immobilizing molecules and the enzymatic system to study. Since the electrode material used in spectroelectrochemical experiments is a metal (gold or silver), SAMs are the common platform used for enzyme immobilization. The spectral overlap between a SAM and a protein is usually negligible since the main signals arising from the alkyl chain are located in the high wavenumber region of the spectra (2800 cm^{-1}–3000 cm^{-1}). However, one has to pay attention to the chemical head group of the SAM, especially amine functions (N–H bending mode of primary amines from 1650–1580 cm^{-1}) and carboxylic functions (C=O stretching mode from 1760–1690 cm^{-1}). This issue is compounded when much more complex modifications of the electrode are required. This problem has been tackled in a very elegant manner for the immobilization of a membrane protein—the bacterial respiratory ubiquinol/cytochrome bo_3 (cyt bo_3) [117]. In this study, a tethered bilayer lipid membrane (tBLM) was used to immobilize cyt

bo_3. The commonly used lipid tether cholesteryl (2-(2-(2- mercaptoethoxy)ethoxy)ethyl)carbamate (CPEO3), which serves as an anchor for the lipid bilayer, contains a carbamate function that strongly overlaps with the protein signals. In this respect, the authors have successfully synthesized a novel molecule WK3SH (dihydrocholesteryl (2-(2-(2-ethoxy)ethoxy)ethanethiol), an IR transparent variant of CPEO3 lacking the carbamate function, thereby suppressing interferences with signals arising from the secondary structure of the enzyme. This effort allowed the challenging monitoring of a transmembrane proton gradient generated by cyt bo_3 catalytic activity.

3.3.2. Enzyme Engineering

Engineering on the enzymes can alternatively serve to tune the interaction between bare or functionalized electrodes. Although very elegant, this strategy has been less employed so far, mainly because it can affect both stability and activity of the protein before and after immobilization. However, unlike nonspecific adsorption where multipoint connections between enzymes and electrodes are possible, site-specific attachment can provide an orientational immobilization that will also dictate the distance between the enzyme active site and the electrode surface [118–120]. The approach can thus maximize the rate of direct ET, with low distribution of ET rates. The basic approach is to use genetic engineering to introduce linkers on the functional proteins, then immobilize these protein molecules on the electrode via the linkers. The electrodes have to be chemically modified accordingly to specifically react with the labeled enzyme.

A classical site-specific immobilization method relies on the introduction of affinity tags like polyhistidine tags (His-tag), which are widely used in biochemistry for protein purification. His-tags have six sequential histidine residues that can chelate metals like Cu, Ni, or Co [121], or can favor the electrostatic interactions towards hydrophilic surfaces [122]. The issue here is to evaluate the effect of such site-specific immobilization of genetically engineered protein molecules compared to random immobilization on the interfacial ET efficiency. With His-tags being quite long linkers, the increased distance may impede the ET, or on the contrary may induce required flexibility of the immobilized enzymes. Oriented immobilization could be obtained via the formation of ternary metal chelate complexes between metalated nitriloacetic acid (NTA), such as a Cu-NTA functionality on the electrode, and His-tagged recombinant proteins. Balland et al. designed a short-length NTA-terminated alkane thiol to immobilize His-tagged LAC on a gold electrode through copper ligandation [121]. Both N- and C-terminal His-tagged LACs were studied with the expectation of a more favorable orientation of LAC through the C-terminal labeling which is closer to the Cu T1. Although catalysis of O_2 reduction was reported in the presence of a redox mediator, no direct current could be obtained even in the most favorable C-terminal modification. This result strongly suggested that His-tag labeling at the C-terminal or N-terminal sequences in LAC does not allow Cu T1 to approach the electrode at a tunneling distance. In another study, deletion of a flexible 10-amino-acid sequence at the C-terminal end of a two-domain-type LAC was performed to expose the Cu T1. Labeling with a His-tag was additionally introduced in the mutated enzyme [122]. The catalytic activity of the wild-type LAC was compared to the mutated one, once immobilized on Au electrodes modified by SAM displaying various chemical functionalities [122]. Direct wiring of the enzymes was achieved and explained by the proximity of the C-terminal end to the Cu T1 in the LAC under study. Despite the fact that no significant difference in the surface concentration between adsorbed WT or mutants exists, direct electrochemical activity was reported to be much higher on mutated enzymes due to the oriented immobilization of genetically engineered enzymes. Li and collaborators introduced a cysteine-6-His-tag either at the C-terminal or N-terminal end of a LAC for an oriented immobilization on gold electrodes. The strategy was based on different distances to the Cu T1 or Cu T2/T3 between C-Ter and N-Ter. Based on the quantification of produced H_2O_2 during O_2 reduction, the authors proposed that a different orientation was obtained depending on the C-Ter or N-Ter grafting. It must be noticed, however, that no clear catalytic signals could be observed in both cases, underlining most probably a slow ET independently

of the immobilization strategy [123]. These three related examples illustrate the difficulty to rationalize the efficient immobilization of engineered enzymes for electrocatalysis.

Other peptides have potential binding properties for different types of surfaces. These peptides are expected to bind to surfaces by noncovalent interaction, and can exhibit high affinity and selectivity [124]. They are mostly selected by the phage display peptide library [125]. Few binding peptides display some affinity for material surfaces of interest for electrochemistry, such as for graphene [126], carbon nanostructures [127], and gold [128,129]. Some peptides are already used to anchor enzymes on different types of surfaces such as alkaline phosphatase on a gold surface [129]. Currently, these peptides are not used to immobilize and orient redox enzymes on electrode surfaces, but they could provide a robust method to bind the enzyme at a different part of the protein. However, this binding method could also suffer from inhibition of the ET because of the length of the linker.

The publications just described above engineered only the N-terminal or C-terminal end. It should be interesting to have possibilities of mutation at other targeted parts of the enzyme, eventually closer to the active site, or at any locations on the enzyme surface in order to relate the position at which the enzyme is immobilized to the ET rate. As a recent illustration, cellobiose dehydrogenase from *Myriococcum thermophilum* has been shown to be an ideal candidate for site-directed mutagenesis. Having no surface cysteine residues, this amino acid was introduced at specific surface locations in view of the oriented immobilization [130]. "Thiol-ene" click chemistry between the thiol group available on the cysteine moieties and vinyl groups grafted on the electrode was successfully exploited for site-specific covalent linkage. The cysteine moieties were introduced on the dehydrogenase domain in such a way that two different orientations of the active site (the heme group of the flexible cytochrome domain) were ensured upon immobilization. An increase in electrocatalytic activity in terms of current for site-directed covalent immobilization was reported compared to physical adsorption, in a ratio ~7, thus indicating favorable enzyme loading on the electrode. Interestingly, a significant difference in current output was also observed between the two different grafting localizations, suggesting a control of the orientation of the enzyme. In the same way, a fungal laccase presenting a unique surface lysine residue close to the T1 Cu site was immobilized on planar electrodes [131]. This strategy can be applied in all the cases where a unique surface residue can be genetically engineered. However, site-specific protein engineering is sometimes limited by the available sites on the protein surface and/or because such modifications might alter the function or structure of the protein. Homology modeling can also be used to design new mutants with enhanced catalytic activity and immobilization yield on a surface. This was the case in the work of Gao et al. who performed site-directed mutagenesis on formate dehydrogenase immobilized on nanoparticles [132].

An attractive new strategy is the use of noncanonical amino acids (ncAAs) like propargyl-L-lysine (PrK), which can be genetically introduced at desired locations on the enzyme [133] (Figure 6). Moreover, a unique alkyne chemical handle of ncAAs will ensure a covalent linkage of the mutated enzymes with the modified electrode via click chemistry [133]. By varying the length and position of the linker on the *E. coli* CueO, the distance of the enzyme's electroactive site relative to the glassy carbon electrode was controlled [134]. It was shown that (i) site-directed anchorage was more efficient for direct O_2 reduction than nonspecific immobilization; and (ii) labeling far from the active site was not favorable to high catalysis efficiency. However, it was also emphasized that the ET efficiency was not directly related to the distance between the active site and the electrode, suggesting that other pathways such as ET through the structure of the protein may be involved. In that particular study, one can wonder whether the flexibility of the linker could be a major factor governing the overall ET.

The effectiveness of oriented immobilization and electrochemical operational stability for these genetically modified enzymes on electrode surfaces certainly depends upon the immobilization strategy. In case of chelation between a histidine moiety on the modified protein and Cu–NTA ligands on the electrode, stability can be affected by dissociation of the Cu ion from the NTA-modified electrodes induced by competitive binding with the His-tag on the enzyme [135]. In comparison,

the operational stability of bioelectrodes prepared by covalent conjunction using click chemistry between cysteine-modified protein and vinyl groups of the electrode lasts up to a few days [130].

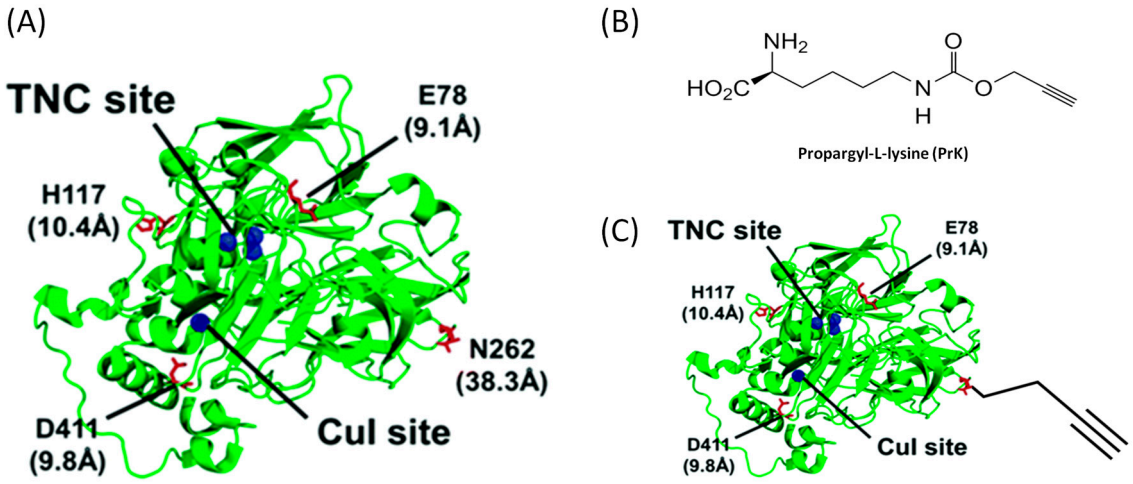

Figure 6. (**A**) 3D structure of cuprous oxidase (CueO) including the two redox centers (blue spheres). The four noncanonical amino acids (nCAAs) incorporation sites are labeled in red; (**B**) Chemical structure of Propargyl-L-lysine (PrK); (**C**) Genetically modified enzyme offering a unique alkyne moiety for site-specific attachment to electrodes via click chemistry [134].

4. How to Probe Enzyme Orientation on an Electrode

4.1. Electrochemistry

Electrochemical techniques are the ideal tools to study both intramolecular ET within an enzyme and interfacial ET between the enzymes and the electrodes. Theoretically, using cyclic voltammetry and chronoamperometry, kinetic parameters of the catalysis can be quantified. However, the type of kinetic data which can be obtained is linked to the type of interaction between the enzyme and the electrode, and especially to the enzyme's orientation [136]. Enzyme/electrode interaction is of utmost importance because the ET rate is exponentially dependent on the distance between the redox active center and the electrochemical interface, as predicted by the Marcus theory [24,137]. Fifteen years ago, most electrochemical studies involved the enzymes in combination with their physiological partners, or artificial redox partners, either diffusing or co-immobilized with the enzymes [138]. Unlike the observation of the redox signals for small proteins such as cytochrome *c* or ferredoxins [139], it was thought at that time that the size of the enzyme and the burying of the active site would preclude any direct electrical connection. Instead, the redox partners play the role of electron shuttles between the active site and the electrode, in a similar way as they are doing physiologically. Then, the so-called mediated catalytic current (MET) gave access to second-order rate constants between many different redox enzymes and their partners, and also allowed the demonstration of pseudo-specificity of the catalysis [140]. However, such a mediated electron transfer system has several disadvantages in terms of thermodynamic loss between the mediator and the enzyme, decreased efficiency due to potential mediator leaking, and difficulty to design a simplified system. The increasing knowledge of the arrangement of the active centers, of the cofactors, and of the distribution of surface charges and hydrophobic patches for an increasing number of redox enzymes has allowed the determination of the key parameters for their favorable orientation on functionalized electrodes. Hence, a direct electrical connection (DET) can be achieved, although many redox enzymes are still electrochemically silent. In some cases, the determination of the surface coverage of the enzymes participating in the catalysis, then the quantification of the catalytic constant k_{cat}, Michaelis constant (K_M), or inhibition constants was achieved [141]. This advanced analysis is mostly observed, however, on nanostructured

electrodes, such as carbon nanotube- or gold nanoparticle-modified electrodes, that are able to enhance the loading of enzymes, thus increasing the detection signals. Interestingly, studying the MET/DET ratio appears to be relevant for the evaluation of the distribution of the orientation of the enzymes on the electrode [136]. In addition, being a relative value, the MET/DET ratio is free from errors caused by the variation of adsorbed enzyme amount [30]. This strategy was applied to various enzymes immobilized on thiol-based SAMs and allowed to determine the surface chemistry on the electrode able to promote DET. One can cite relevant studies that analyzed the catalytic efficiency of *A. aeolicus* [NiFe]-Hase [142] on negative, positive, or hydrophobic SAMs on gold, of *D. gigas* Hase on positive SAM on gold [143], of *R. eutropha* [NiFe]-Hase on negative SAM on silver [61], of *Trametes hirsuta* LAC on neutral hydrophobic SAM on gold [144], of *Cerrena unicolor* C139 LAC positive SAM on gold [107], or of *Myrothecium verrucaria* BOD on positive or negative SAMs on gold [145] (Figure 7). In the latter paper, electrochemistry was coupled to SPR demonstrating that the switching between DET over MET when adsorption was performed either on negative or positive SAM was effectively linked to a different enzyme orientation and not to different enzyme loading. A similar study based on the coupling between electrochemistry and QCM to investigate O_2 reduction catalysis by *M. verrucaria* BOD further concluded with an optimum enzyme density on the SAM–Au electrode for direct catalysis [146].

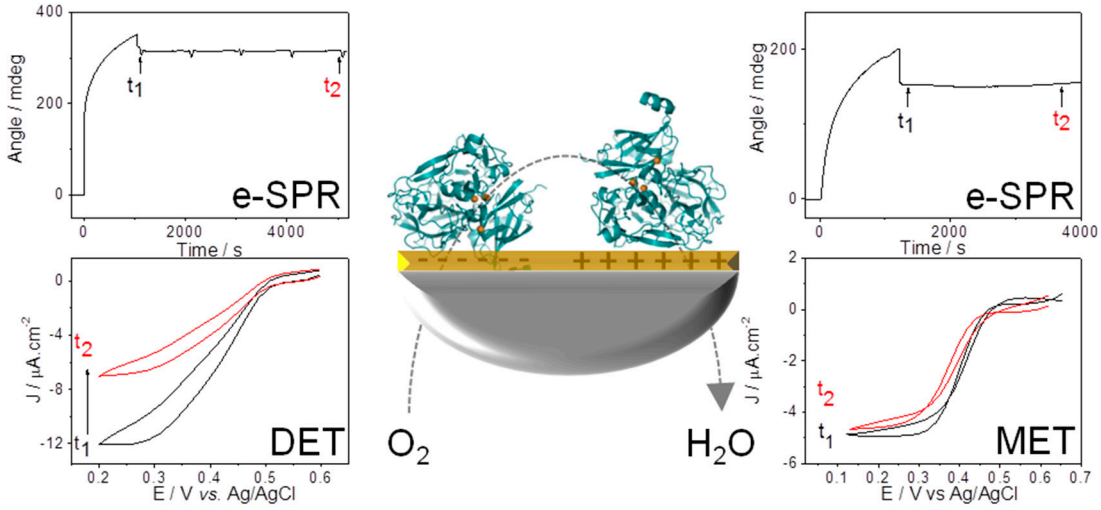

Figure 7. Coupling SPR with electrochemistry allowed the demonstration of a different orientation of the *M. verrucaria* bilirubin oxidase (BOD) according to the charge of the electrode controlling the type of ET process for enzymatic O_2 reduction. On either positive (**Right**) or negative (**Left**) SAM-modified gold electrodes, surface adsorption of the enzyme is successful. However, negatively charged SAM (**Left**) allows direct ET (DET), while positively charged SAM (**Right**) requires a redox mediator for catalysis (MET). Adapted from [145].

4.2. Spectroscopies

Thanks to specific surface selection rules [147], infrared techniques such as SEIRA and IRRAS spectroscopies have been successfully used in order to evaluate the orientation of redox enzymes immobilized onto electrodes. In those methods, the electromagnetic field propagates in a perpendicular direction to the metal surface. Therefore, the chemical groups with a dipole moment oriented perpendicular to the metal surface will exhibit the highest intensity of IR absorption, whereas the ones with a dipole moment parallel to the surface will show no absorption at all. For dipole moments lying in between, the intensity of the IR signal will depend on its angle with the surface normal. In proteins, the main secondary structure elements are α-helices and β-sheets, associated with specific amide I (C=O stretching mode, N–H bending) and amide II (combination of N–H bending and C–N stretching) spatial arrangements. Consequently, while the amide I dipole moment of an α-helix lies parallel to the

α-helix itself, its amide II component is perpendicular. For β-sheets, the situation is reversed for the main amide I and amide II components. As a consequence of this surface selection rule, the intensity ratio between Amide I and Amide II bands brings information regarding the orientation of the enzyme provided that a structure or a model of the enzyme is available [148] (Figure 8).

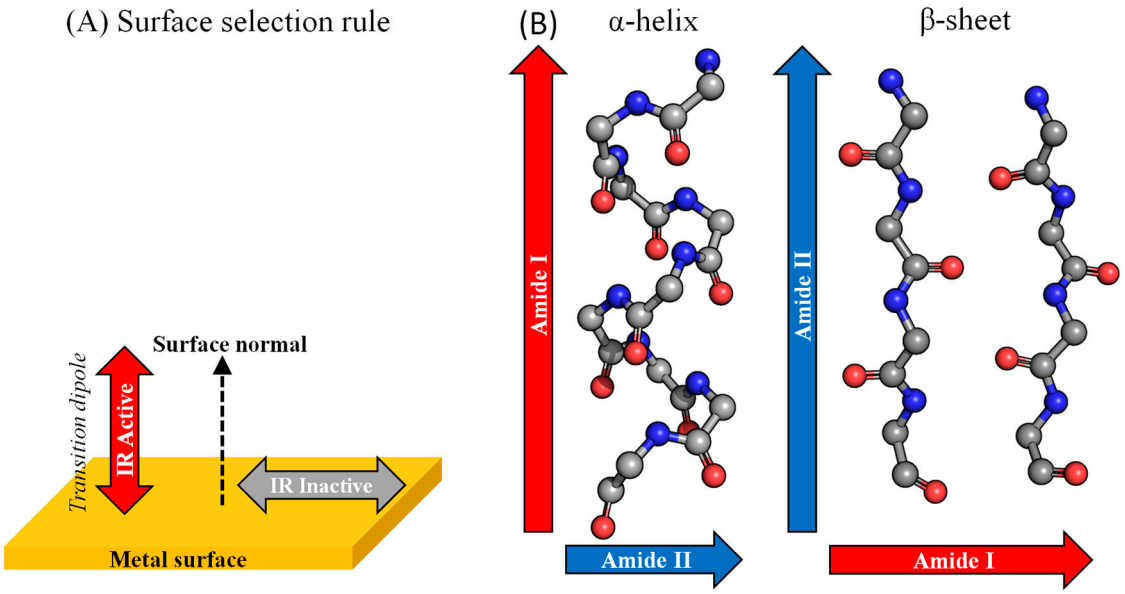

Figure 8. (**A**) Scheme representing the surface selection rule. Molecules with a transition dipole moment perpendicular to the metal surface exhibit the highest IR intensity while the parallel ones show no IR absorption; (**B**) Backbones of α-helix and β-sheet secondary structure elements with C=O and C–N highlighted in red and blue, respectively. Arrows show the direction of dipole moment depending on the type of chemical bond—amide I or amide II—relative to the secondary structure.

Surface-Enhanced Infrared Absorption (SEIRA) spectroscopy was used in combination with MD simulations to observe and rationalize the immobilization in a controlled orientation of membrane-bound [NiFe]-Hase from *Ralstonia eutropha* [149]. The membrane-bound Hase from *D. vulgaris* Hildenborough was reconstituted onto a SAM-modified gold electrode with a subsequent addition of a lipid membrane, either below or above the enzyme [150]. Immobilization on top of the membrane led to a great freedom of movement of the immobilized enzyme as indicated by the wide variation in the ratio of amide I to amide II between reproduced experiments. In the other configuration with the enzyme below the membrane, the direct interaction between the enzyme and the SAM-modified gold electrode led to a ratio of amide I to amide II close to 1, reproducible between experiments, indicating a more uniform immobilization procedure. Similarly, the different orientations adopted by a LAC depending on its covalent or noncovalent binding to the electrode [144] were monitored by SEIRA spectroscopy.

Polarization Modulated Infrared Reflection Absorption Spectroscopy (PM-IRRAS) allowed the observation of different orientations of the membrane-bound Hase of *A. aeolicus* [142]. Indeed, depending on the physico-chemical properties of the SAM-modified gold electrode (hydrophilic or hydrophobic), the intensity of the ratio of amide I to amide II varied, reflecting different orientations of the enzyme. Moreover, on the basis of simulations, those ratios could be correlated to the angle of the α-helices (main secondary structure element) present in the enzyme with respect to the normal of the electrode, giving an idea of the absolute orientation of the enzyme. Those results provided a structural interpretation of the electrochemical behavior of *A. aeolicus* Hase alternating between pure MET or a mixed DET + MET process depending on the physicochemical properties of the electrode. Similarly, PM-IRRAS was used to study the orientation of LAC onto SAM-modified gold electrodes depending on

the charges of the SAM headgroup [107]. Different orientations correlated with electrochemical signals were observed with significantly higher catalytic signal for LAC immobilized on positively charged surfaces. The same authors studied various immobilization procedures comprising hydrophilic SAM (mercapto ethanol), lipidic SAM (Dipalmitoylphosphatidylglycerol), and charged diazonium salts. They were able to conclude that orientations of LAC with β-sheets lying parallel to the electrode were associated with electrochemical response for O_2 reduction [151]. BOD from *M. verracuria* BOD was recently studied in a combined study including PM-IRRAS [145]. Despite drastically different electrochemical signals for O_2 reduction depending on the charges of SAM-modified electrodes, similar spectral features were observed for the amide region. This apparent discrepancy was rationalized on the basis of the particular topology consisting of a repeated β-barrel motif in the *M. verracuria* BOD.

4.3. Microscopy

Studying protein orientation with AFM [152] was proposed quite early, though in an indirect way. Using antibodies that bind to a specific region of the protein and measuring the volume of the protein/protein complex allows us to decipher if the antibody is present and, therefore, to deduce the orientation of the protein. Similarly, measuring by AFM the height profile of the protein-modified electrode after incubation in an antibody solution could also indicate the presence or absence of antibody, and therefore give clues about the protein orientation. However, if this technique has sometimes been used for simple redox proteins, to the best of our knowledge this has never been applied to enzymes. On the other hand, very few studies report the use of microscopy for direct evaluation of enzyme orientation. Actually, the direct measure of height profiles by AFM without antibody is a valuable method only if one dimension of the enzyme is characteristic. Hence, no information about the orientation can be obtained when globular enzymes are studied. LAC immobilization on mixed SAMs was, for example, studied using AFM, which gave information regarding enzyme distribution on the electrode surface. However, since these enzymes are recorded as quasi-spheres, the method would not be useful to determine their orientation [153]. In another example, *A. aeolicus* membrane-bound Hase immobilized on hydrophobic SAM was examined with AFM. Once again, approximately 3 nm high spherical features were observed, thus indicating the presence of a monolayer of enzyme but not which orientation was adopted [142]. A similar result was obtained with another globular enzyme—*R. eutropha* membrane-bound Hase—immobilized on a gold electrode [149].

However, an STM study, as well as three examples where AFM proved useful in determining enzyme orientation, are worth mentioning. The cytochrome *c* nitrite reductase from *E. coli*, a decaheme-containing homodimer with asymmetric dimensions, was adsorbed at an Au (111) electrode. STM was used to measure the lateral dimension of the immobilized enzymes and thus inform about their orientation [154]. This approach demonstrated that a distribution of orientations is adopted and that the enzymes possibly immobilize as monomers and dimers. A recombinant horseradish peroxidase bearing His- or Cys-tags at different positions with respect to the heme active site was attached to a gold electrode via the tag [155]. AFM measurements were performed in liquid (in 150 µL PBS), i.e., in an environment able to preserve the enzyme native structure (as far as it can be preserved on a solid surface). Various height profiles of the tagged proteins were measured on an Au (111) surface, indicating that different binding points lead to different orientations of the proteins. Furthermore, this observation was consistent with the different heterogeneous ET rates between enzyme and electrode recorded in electrochemical experiments.

The orientation of the [NiFeSe] membrane-bound Hase from *D. vulgaris* Hildenborough on a gold electrode modified with SAMs and a lipid bilayer was further studied by combining AFM and electrochemistry [156]. This Hase is characterized by the presence of a lipidic tail at the opposite of the distal 4Fe4S cluster—the exit point of electrons. The enzyme is elongated and the longest dimension corresponds to the axis 4Fe4S cluster-lipidic tail. When the electrode, first modified with SAMs and a lipid bilayer, was incubated in a Hase solution, AFM showed the apparition of globules whose height

suggested that the Hase's longer dimension was vertically oriented. This orientation happened only when the lipidic tail was present, and not when the soluble form of the enzyme was studied instead. Since only MET was possible in electrochemistry, this observation indicated that the lipidic tail was inserted in the lipid bilayer. On the contrary, when the electrode was co-incubated in a solution of Hase and phospholipids, AFM indicated a flat surface with deep holes. After dissolution of the lipid bilayer with surfactants, globular features corresponding to Hase molecules were recovered. Since in this second case DET was allowed, the 4Fe4S was supposed to be oriented towards the electrode, while the Hase lipidic tail was inserted in the lipid bilayer on top of it. The same enzyme was combined with *E. coli* F_1F_0 ATP-synthase inserted in the lipid bilayer overhanging it. This whole machinery allowed the use of H_2 as a fuel to produce the proton gradient necessary for ATP synthesis. The F_1F_0 ATP-synthase consists of a large soluble domain and a smaller membrane domain. The presence and the size of protrusions on top of the lipid bilayer recorded by AFM indicated a unique orientation of F_1F_0 ATP-synthase with its soluble domain directed towards the outer of the membrane [157].

Finally, the bacterial respiratory complex I from *Rhodothermus marinus* was reconstituted in a biomimetic membrane on a gold electrode. The complex is a single protein (NADH-menaquinone oxidoreductase) consisting of two L-shaped domains [158]. The complex in its native form was first inserted in liposomes before incubation of the SAM-modified gold electrode in the proteoliposome suspension. A lipid membrane with protrusions of 6–8 nm was evidenced by AFM. This distance is consistent with the hydrophilic part of the protein extending outside the lipid membrane, although the size is smaller than that evidenced by X-ray crystallography (13 nm), suggesting that the L structure is flexible (Figure 9).

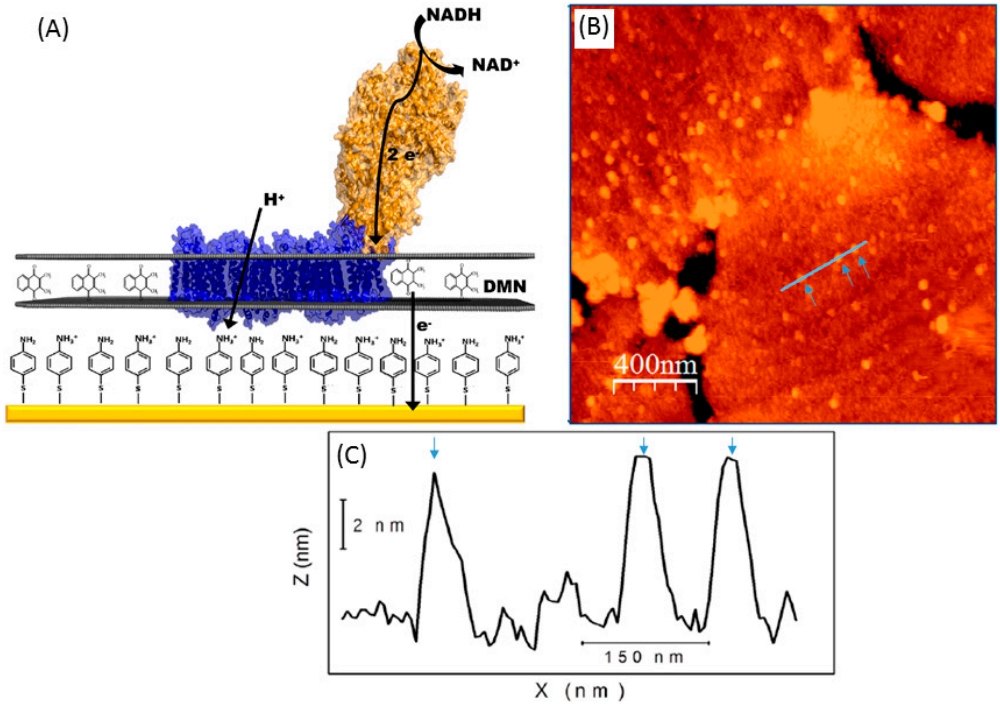

Figure 9. AFM study of the NADH-oxidizing respiratory complex I reconstituted in a phospholipid bilayer on a gold electrode. (**A**) Schematic representation of the reconstitution. The gold electrode is modified with 4-aminothiophenol and the phospholipid bilayer contains the redox mediator 2,3-dimethyl-1,4-naphtoquinone; (**B**) Tapping-mode AFM topography of a gold plate modified with 4-aminothiophenol to which complex I has been immobilized; (**C**) Z-axis profile across the line drawn in (**B**). The arrows indicate features whose height corresponds to the arm of complex I protruding outside the membrane (yellow structure in (**A**)). Adapted with permission from [158].

4.4. Modeling

To study functionalized electrode surfaces for enzyme immobilization, modeling approaches offer a window into the detailed surface interactions at the molecular level [28]. Several approaches can be used to predict the preferred orientation of enzymes on surfaces by modeling. SAM-functionalized gold surfaces have been modeled in numerous simulation works on enzyme–surface interactions, for example, to probe the enzyme binding orientation as a function of the surface charge [149]. Matanovic et al. used a combination of Density Functional Theory (DFT) and docking simulations to study the oriented interaction between bilirubin oxidase and a graphene electrode functionalized with bilirubin [159].

Sampling all relevant configurations sufficiently is one of the inherent challenges of such methods. ProtPOS (Prediction of Protein Preferred Orientation on a Surface) is software designed to predict the preferential orientations of a protein adsorbed on a surface. Its approach is to search for low-energy protein–surface conformations [160]. The use of a particle swarm optimization (PSO) algorithm allows fast computation of the energies of protein poses in every rotational and translational degree of freedom of the protein–surface complex [161]. The stochastic character of the PSO algorithm makes several runs necessary, with each run returning the lowest energy orientation of the protein on the surface that can be fed into MD simulations with a wide range of software—such as GROMACS [162] or AMBER [163,164].

More generally, the search for a global minimum in the enzyme–surface interaction energy landscape is a classic way to handle the question of protein orientation on a surface [165], and can be addressed via several modeling schemes such as parallel tempering Monte Carlo [166], docking via Brownian Dynamics Simulations [167], or MD simulations [168]. In their recent study on β-galactosidase grafted on a hydrophilic surface, Li et al. used coarse-grain MD simulations to probe the enzyme orientation and its catalytic activity as a function of the surface's hydrophilicity [169]. Such coarse-grain approaches have been developed for modeling protein–surface interactions because they allow an increase in the time and length scales that are accessible during simulations [28]. While coarse-grain representations can successfully address issues such as proteins binding on surfaces [161], or folding [32], they are, however, unable to deal with oxido-reduction processes and could not be used to describe ET between surfaces and enzymes until now.

When enzymes are immobilized on a surface via covalent bonds, for example, in the case of laccase bound on a SAM-functionalized gold surface, one can also determine the enzyme orientation by identifying the protein surface residue that will form the lowest energy bond with the SAM via calculations [169]. Bioinformatics tools represent another useful approach to determine a suitable orientation for enzymes immobilized on a surface in order to promote direct electron transfer, for example, by identifying hydrophobic patches on the protein surface [170].

5. Factors Driving the Oriented Immobilization at an Electrode

5.1. Importance of Electrostatic Interactions to Drive the Oriented Immobilization for Fast ET

As discussed in Section 3.1, electrostatic interactions are a major factor governing the stabilization of physiological protein–protein or protein–substrate interactions. In the context of intermolecular ET, it is therefore an essential parameter that needs to be evaluated and controlled in order to induce a proper orientation for an efficient electron transfer. Those interactions should inspire and guide the bioelectrochemist willing to achieve a physiological-like protein immobilization. Thus, when a molecular structure of the redox enzyme is available, calculations of the dipole moment of the enzyme might give hints for a rational approach to immobilize the targeted redox enzyme. In cases where the enzyme has a strong dipole moment, the preferential adsorption orientation can be predicted based on the surface chemistry of the electrode [171], while enzymes with less stable dipole moments can display several stable adsorption orientations [149]. Several computational studies on [NiFe]-Hases from various species have highlighted the importance of the enzyme dipole for

determining its orientation on a charged electrode [149]. In particular, the weak, fluctuating dipole moment in the membrane-bound [NiFe]-Hase from *A. aeolicus* enables the enzyme to adsorb efficiently on both negatively and positively charged surfaces [172]. BODs and LACs have been the subject of many studies highlighting the role of dipole moments in their oriented immobilization. For example, the orientation of laccase from *T. versicolor* adsorbed on charged SAMs was shown to be controlled by the enzyme's dipole moment and the distribution of charged patches all over the protein surface [173] (Figure 10).

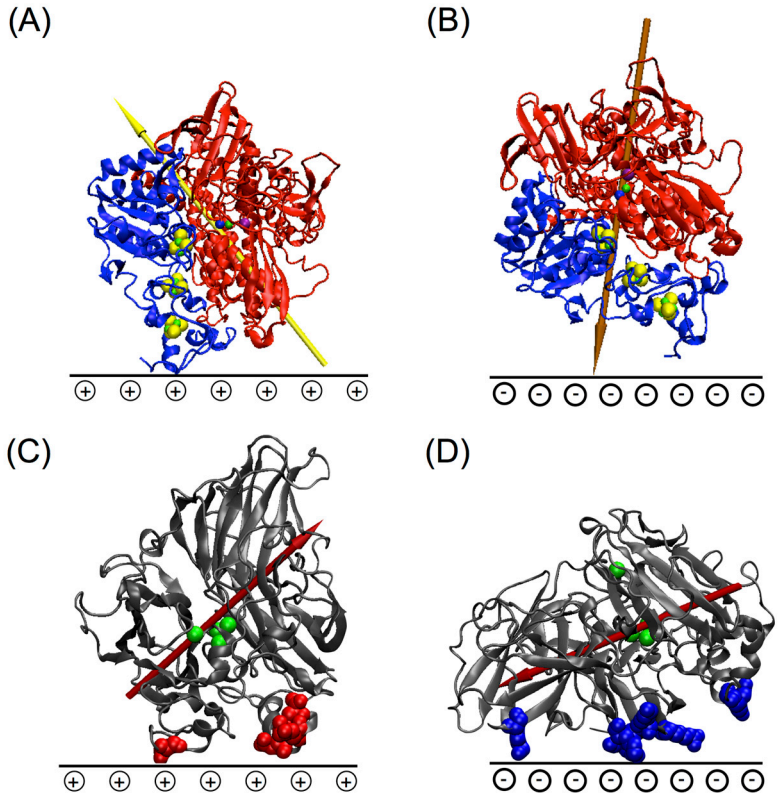

Figure 10. The fluctuating dipole moment of the [NiFe]-Hase from *A. aeolicus* enables it to adsorb efficiently on both positively and negatively charged surfaces (panels (**A**) and (**B**), respectively) [172]. On the other hand, the strong dipole moment in the LAC from *T. versicolor* leads to different enzyme orientations on positively and negatively charged surfaces (panels (**C**) and (**D**), respectively) [173]. Negatively charged residues interacting with the surface are shown as red van der Waals spheres in panel (**C**), while positively charged residues are shown in blue in panel (**D**).

The oriented immobilization on electrode surfaces presenting different charges of two different BODs, one from a fungus (*M. verrucaria*) and the other from a bacterium (*Bacillus pumilus*), was shown to be controlled by the variation of their dipole moments as a function of pH [30]. Hence, direct connection of *M. verrucaria* BOD was obtained upon adsorption at pH 6 on negatively charged surfaces, in relation with a dipole moment pointing towards the T1 Cu, while only mediated catalytic current was obtained on positively charged surfaces [145]. On the contrary, *B. pumilus* BOD, with a dipole moment directed toward the opposite side of the T1 Cu in all the pH range, was unable to achieve any direct connection on negatively charged surfaces. This last example clearly demonstrates that the dipole moment is the key property driving the orientation, much more than the global surface charge which is similar for the two BODs.

Electrostatic control of the orientation of enzymes was reported in other papers, although a direct link with dipole moments was not underlined. Modeling studies highlight the crucial role played

by the surface charge for effective reactions at the interface. For example, the hexameric tyrosine coordinated protein (HTHP) will adsorb in a nonproductive orientation for DET on positively charged SAMs [174]. In their work on sulfite oxidase adsorbing on SAMs, Utesch et al. showed how the solution ionic strength impacts the enzyme adsorption [175]. High ionic strengths tend to inhibit the interaction between the cyt b_5 domain and the SAMs both by competitive adsorption between ions and the cytochrome units, and by the shielding of the electrostatic attraction between the enzyme and the surface. The same group also investigated the effect of the protonation degree of the SAM surface on the immobilization of a [NiFe]-Hase [171]. They showed how the number of contacts between the SAM and negatively charged areas on the enzyme surface increase with the SAM ionization level. The strength of the enzyme/surface interaction is proportional to the SAM degree of protonation. However, MD simulations show that a high (50%) protonation degree of the SAM induces conformation changes in the enzyme that might be detrimental to its catalytic activity. However, one should note that, from a simulation perspective, the vast majority of modeling studies dealing with protein–solid surface systems concerns peptides grafted on surfaces, while the larger, more complex redox enzymes have, until now, attracted much less attention. Electrochemistry was thus the main method used throughout. Ulstrup et al. extensively studied the electrochemical behavior of four MCOs (three LACs, i.e., *Coprinus cinereus* (CcL), *Myceliophthora thermophila* (MtL), and *Streptomyces coelicolor* (ScL) as well as BOD from *M. verrucaria*) on different SAMs terminated by methyl, carboxylate, and amino groups [176]. A clear DET signal for catalytic reduction was reported for *M. verrucaria* BOD and CcL immobilized on negative carboxylate SAMs, and for ScL immobilized on positive or hydrophobic SAMs. No catalytic current could be obtained for MtL on any SAMs. Such observations demonstrate the clear sensitivity of a given enzyme to the local chemistry of the electrode surface more likely due to their electrostatic interactions. Enzymes having negative (ScL) or positive (*M. verrucaria* BOD, CcL) surface charge around the copper T1 active site are adsorbed on positive or negative SAMs, respectively, in a DET-type orientation derived by electrostatic interactions between opposite charges. Hydrophobic interactions have also featured for ScL immobilization on octanethiol SAMs, typically due to the hydrophobic environment around the active site along with negative surface charges. Although MtL is structurally similar to *M. verrucaria* BOD, no clear DET on any SAM surface indicates an entirely different environment around the Cu T1. Oriented immobilization of a [FeFe]-Hase from *Clostridium acetobutylicum* having large positive surface regions was achieved at negative SAMs on gold electrodes [177]. On the contrary, an oxygen-tolerant [NiFe]-Hase from *R. eutropha* adopted favorable orientation for DET-type electrocatalysis on 6-amino-1-hexanethiol coated gold electrodes [149]. This Hase being homologous to *A. aeolicus* Hase, one can suspect that the dipole moment of the enzyme may explain such a result.

5.2. Effect of Covalent Attachment

Covalent attachment is viewed as a general solution to avoid enzyme leaching from the electrochemical interface. The presence of amino, carboxylate, or hydroxyl groups within the amino acid moieties of an enzyme is exploited for covalent binding. SAMs on gold also offer a variety of terminal chemical functionalities that permit ease of covalent conjunction. For covalent attachment, carbodiimide chemistry is the most popular one, where water-soluble 1-(3-dimethylaminopropyl)-3-ethylcarbodiimide hydrochloride (EDC) and N-hydroxysuccinimide (NHS) reagents are commonly used [178,179]. The issue here is whether the covalent attachment will preclude any specific orientation of the enzyme, and hence decrease the ET efficiency. Actually, covalent attachment may result in multipoint attachment of the enzyme as more than one surface functional group may participate during bond formation. Consequently, the relative position achieved by immobilized enzymes is random and enzymes adopt nonuniform distribution orientations.

Infrared spectroscopy is a valuable tool to monitor the formation of a covalent bond between an immobilized enzyme and a linker. The EDC/NHS coupling reaction catalyzing the formation of amide bonds between the amino groups of a linker molecule on the surface of the Au electrode and

the carboxylic acid groups of a LAC was performed [144]. As a result of this covalent attachment, an absorption band appeared at 1737 cm^{-1}, typical of a carbonyl group, confirming the formation of covalent amide bonds between the amino-terminated linker of the gold electrode and the carboxylic functions of the LAC exposed to the solvent. Surface-Enhanced Raman Scattering (SERS) was used to monitor the covalent attachment of the azido-modified horseradish peroxidase onto gold electrodes modified with an alkynyl complex—1,4-dialkynylbenzene (DEB). The success of the click chemistry reaction was evidenced by the disappearance of the azide band of the enzyme involved in the covalent bond with the DEB monolayer [180]. Rudiger et al. reported higher operational stability compared to adsorbed enzymes when *D. gigas* [Ni-Fe]-Hase was covalently attached to gold electrodes modified with a SAM of 4-aminothiophenol. After 80 h of continuous operation, 25% of the initial current was maintained. A clear DET signal confirmed that the immobilization method favors an orientation where the active site of the enzyme faces the electrode surface [143]. Gutierrez-Sanchez et al. reported similar higher operational stability for covalent conjunction of *M. verucaria* BOD to gold electrodes modified by carboxylate-terminated SAM [145]. This result was obtained by coupling SPR to electrochemistry, and was unexpected since it was also demonstrated that before covalent attachment, the decrease in the catalytic signal was not related to any enzyme desorption from the gold surface. This observation clearly demonstrates that covalent binding induces some rigidification of the structure which is favorable to enzyme stability once immobilized. However, with the same *M. verucaria* BOD enzyme and on the same type of negative SAM on gold, Blanford et al. did not find any improvement of stability of the catalytic signal after covalent linking, and even showed a decrease in the magnitude of the current [181]. Actually, characteristics of the immobilized systems, including surface coverage, electrocatalytic activity, and stability of the proteins are considerably affected by the type of bond formed between electrode and protein, which is driven by the immobilization method. In the two cases just reported, the binding reaction was performed in two different ways. In the first case, the enzyme was first oriented according to electrostatic interaction on the SAM-modified gold electrode, and then the coupling reaction was performed. In the second case, the activated ester was first immobilized on the gold electrodes before enzyme coupling.

5.3. Effect of Enzyme Partition

In vivo, catalytic reactions mostly occur in an enzyme-crowded environment. It can thus be suspected that the density of enzymes on the electrode interface might impact the catalysis efficiency. The enzyme surface packing on the electrode could also influence its redox potential. For example, MD simulations and quantum calculations performed on cytochrome *c* covalently bound on a bare gold surface have shown that crowding of the proteins can raise their redox potential to around 100 mV [182]. This effect would be due to the change in the polarizability of the enzyme's environment, where much less polarizable proteins replace water. Concomitantly, enzyme surface density may alter enzyme orientation because of interactions between neighboring molecules. At the same time, such interactions may impede important functional movements. McArdle et al. used electrochemistry coupled to QCM with dissipation analysis to explore the effect of *M. verucaria* BOD molecular density on catalytic activity and layer rigidity. An optimum concentration of enzymes to be adsorbed was found as a balance between rates of adsorption, enzyme denaturation, and reorientation [146]. One way to vary the enzyme density at planar electrodes is to use mixed SAMs composed of different thiol derivatives. These SAMs are usually prepared by co-adsorption from a solution containing different thiol components onto an electrode surface. Mixed SAMs present stronger overall polarization than pure SAMs as a consequence of antiparallel orientation of dipoles within the SAM. In case of electrostatic binding of enzymes, this polarization induces an enhanced amount of enzyme loading [183]. Many studies dedicated to enzymatic electrocatalysis use mixed SAMs, although the partition of the thiols in such mixed layers is not straightforward, and a detailed relationship between the SAM mixed chemistry and the enzyme activity is rarely provided. Actually, dilution of two different thiols may result in homogeneous [184], or phase-separated monolayers [185]. It is

noteworthy that Traunsteiner et al. used electrochemistry to study the effect of the structure of a mixed SAM obtained by the dilution of short-chain thiols with a longer thiol chain, the linker, on the binding and catalytic efficiency of *T. versicolor* LAC (Figure 11). The linker was chosen to fit the Cu T1 pocket and to bind LAC in a favorable orientation for electrocatalysis. The arrangement of the linker was visualized by high-resolution STM, showing two configurations as a function of water content in the thiol solutions. In case of separated domains of the linker and the short thiol chain, very small catalytic current was observed, contrary to the high current obtained when LAC was immobilized on homogeneous mixed SAM. In the latter case, it was suggested that the isolation of the linker by short thiol molecules improved the binding of LAC [153].

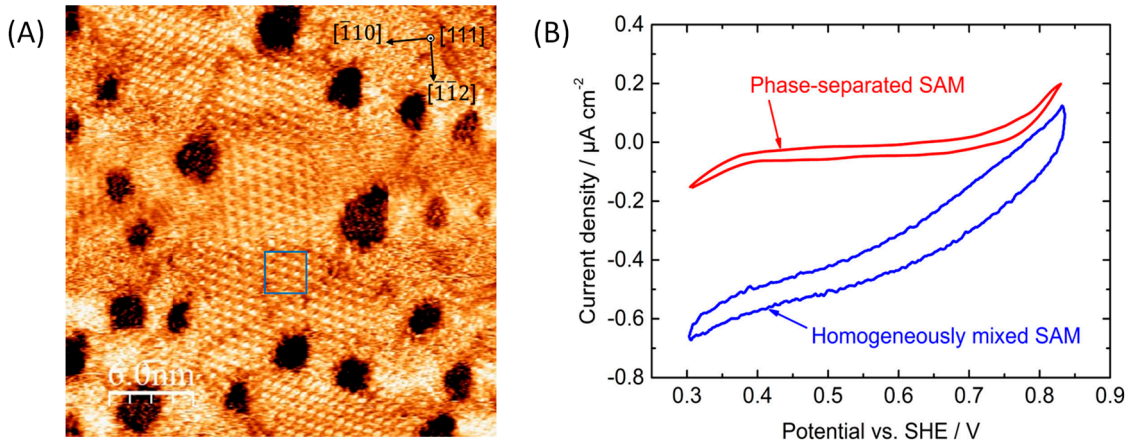

Figure 11. (**A**) EC-STM image showing homogeneous phase of a mixed SAM on Au(111) and (**B**) CVs of *T. versicolor* LAC immobilized on the homogeneously mixed SAM (blue) and the phase-separated SAM (red) on Au(111) in oxygen-saturated solution [153].

5.4. Effect of Potential, Electric Field

Electrical potential is a major parameter which controls redox enzyme activity, but also the formation of inactive states, or reactivation processes, by modulating the redox state of the active site. In addition to electrostatic interactions between charged species (either electrode or enzyme) induced by pH-dependent surface chemistry, electrical potential may also influence the enzyme conformation and orientation (and, hence, catalysis) in two different ways. First, performing the adsorption of the enzyme under an applied potential may have an impact on the orientation by creating an electric field around the enzyme. Second, imposing a potential once the enzyme is adsorbed on an electrode surface should affect its orientation and even its conformation by changing the charge in the environment of the enzyme. These two processes have been explored in only rare papers.

Proteins can be divided into hard and soft proteins depending on the conformational entropy of their structure. It was shown by ellipsometry and MD simulations that soft proteins, such as glucose oxidase, are less sensitive to changes in the conformation under applied potential once immobilized on a solid surface [186]. CueO [187] and fructose dehydrogenase (FDH) [188] adsorbed on a bare gold electrode at potentials around the potential of zero charge (E_{pzc}) showed the highest direct catalytic activity, suggesting a more favorable enzyme orientation. For both enzymes, DET activity decreased when enzymes were allowed to adsorb at electrode potentials far from the E_{pzc}. Different behavior as a function of the adsorbed potential was observed depending on the surface of the gold electrode, either bare, or modified by a hydrophobic thiol layer. The proposed model explains how the electrostatic interaction between the enzymes and the electrode in the electric double layer affects the orientation, but also the stability of the adsorbed enzymes. Lopez et al. immobilized *M. verrucaria* BOD on bare and nanocrystalline gold electrodes via potential pulse-assisted immobilization [189].

An increase in the direct catalytic current was observed compared to the electrode simply prepared by drop casting of enzyme, likely from a preferential orientation of *M. verrucaria* BOD.

The effect of electrode potential on protein immobilization after enzyme adsorption has also been investigated. Change in enzyme orientation upon application of a potential on the membrane-bound Hase from *R. eutropha* was monitored by spectroelectrochemistry [149]. Indeed, as discussed above, application of a negative potential below the E_{PZC} of the SAM-coated Au electrode confirms a reorientation of a fraction of the enzyme population in a more favorable configuration for DET, leading finally to an increase in catalytic current. On the other hand, possible deleterious side effects induced by the application of potential have been evidenced [190]. In the case of the anaerobic [NiFe]-Hase from *D. vulgaris* Miyazaki F, continuous potential application leads to a decrease in the intensity arising from the infrared markers of the active site (one C≡O and two C≡N ligands). Remarkably, the signal intensity arising from amide I and amide II bands reflecting the structural integrity of the enzyme remains constant, suggesting a targeted destruction of the active site. The authors suggest the in situ generation of ROS reacting with the active site and leading to its destruction. This experimental dataset argues against the widely used "film loss" explanation. Besides this, catalytic current dependence on the electrochemical methods used emphasized that cyclic voltammetry induced a faster decrease in the current for O_2 reduction by *M. verrucaria* BOD with time than did chronopotentiometry, suggesting a clear influence of the applied potential on the current stability [181]. The interfacial electric field has also been pointed out to affect the redox potential of enzymes. A SEIRA study of the type II NADH: Quinone Oxidoreductase from *E. coli* immobilized on SAM-modified gold electrodes outlined a substantial increase in the redox potential of the enzyme (~140 mV) [191]. The authors attributed this upshift in potential to an electric-field-driven stabilization of the flavin cofactor. This interpretation was supported by previous similar observations on tetraheme cytochromes c_3 [192].

6. Future Directions: Towards Rational Bioelectrode Design

We have reviewed how to control the orientation of redox enzymes on electrochemical interfaces. This step is mandatory to achieve a fast ET process and maximize the quantity of loaded enzymes on the surface. Success in such oriented immobilization is particularly important for practical applications as it will enable higher sensitivity for biosensors as well as higher current densities—and, hence, power densities—for biofuel cells. Fundamental understanding of the physiological processes in which redox enzymes are involved for ET is essential if one wants to provide the best tailored immobilization procedure. Protein–protein interactions can be investigated using numerous modeling tools, especially to identify potential interaction partners, and to determine the structure of protein assemblies on a surface [193] and the stability over time of these complexes. In particular, the modeling of protein complexes permits the identification of conformational changes induced by protein binding, which are likely to have a noticeable effect on the enzyme's biological function. Key parameters that may yield some degree of control over the orientation of enzymes may be deduced. The molecular bases for functional orientation of common and largely used enzymes are now available. This is the case for BOD and LAC, the enzymes widely used for O_2 reduction. This is also the case for Hases, which have been studied in depth on different types of planar electrodes. However, many enzymes, particularly less broadly used ones, remain silent in electrochemistry, which illustrates that the sole examination of the structure of an enzyme is not sufficient to describe the immobilization and ET phenomenon in its full complexity. The influence of tags used for purification, and surfactants in the case of membrane proteins, may play an essential role in enzyme orientation which is often underestimated.

One important issue that still needs to be further investigated is the effect of the orientation required for DET on the conformation and dynamics of the immobilized enzyme. Electrostatic interactions are most often required to guide a proper orientation of the enzyme yielding a high ET rate constant. Whether these interactions can affect the native conformation, or even denature the enzymes, is still an open question. From a theoretical perspective, molecular modeling approaches provide us

with a detailed picture on the molecular level of how the surface/protein interaction can control the enzymes' orientation, and eventually impact their conformation and internal dynamics. In addition, quantum calculation can help determine potential modifications of the enzymes' redox properties and catalytic activity when they are immobilized on the electrode surface. Some experimental works already clearly state change in the conformation of enzymes upon immobilization on an electrode. As a relevant illustration, the two highly homologous membrane-bound [NiFe]-Hases from *A. aeolicus* and *R. eutropha* display completely different behavior on highly negatively charged electrode surfaces [194]. Recovering of the catalytic signal for H_2 oxidation after surfactant addition in the *R. eutropha* Hase sample suggested that the absence of a surfactant compared to the *A. aeolicus* Hase sample induced structural changes of the enzyme because of the strong electrostatic interactions. LAC and BOD immobilized for DET on gold electrodes were shown to face potential-induced structural changes as revealed by SERRS and ellipsometry experiments [58,141]. QCM and dual-polarization interferometry studies of BOD immobilized on negative SAM-based gold electrodes highlighted that deformation required for DET should lead to a decrease in activity at high enzyme concentrations [146].

To improve the understanding and control of the molecular details involved in protein–electrode interaction, it is now mandatory to develop new methods that are able to relate in real time electrocatalytic activity to enzyme loading, enzyme partition, and enzyme conformation and dynamics. However, very few works nowadays report such coupled methods. One exception is SPR and QCM coupled to electrochemistry, the so-called e-SPR and e-QCM approaches that were already developed to correlate enzyme loading to activity [145,181]. Such coupled methods established for the first time the relation between the amount of deposited enzymes and the enzymatic activity. They also allowed a definite demonstration that a decrease in catalytic currents was not a result of enzyme leaking in most cases, but was due to other processes. Whether these other processes involved are reorientation, change in conformation, or denaturation must be now elucidated. Further developments in orientation-sensitive spectroelectrochemical methods such as PMIRRAS and Plasmon Waveguide Resonance [195], a much more sensitive variant of SPR able to measure affinity and kinetics of interaction, are currently running. They may allow us to relate the conformation of the enzyme or reorientation to its activity. To characterize the overall surface topology, fluorescence microscopy, or AFM approaches, should also be coupled to electrochemistry to constitute a map of enzyme localization on an electrode surface, and visualize the real effect of enzyme density. Such approaches require technological set ups that are currently under investigation for other redox systems than enzymes, but may be applied to redox enzymes in the near future [196]. Sampling issues remain a bottleneck in the simulation of enzyme–surface interactions, in particular, for investigating processes taking place on a large range of length and time scales. Therefore, the development of enhanced sampling methods and multiscale approaches represents a central challenge for studying such complex systems. Finally, sensitive electrochemical methods have to be developed to search for noncatalytic signals, allowing us to access the real amounts of enzymes effectively participating in the catalysis.

With that objective and to enhance the signal-to-noise ratio, electrochemical interfaces other than planar electrodes should be used. However, one should define for which conditions the key parameters for a specific enzyme orientation obtained on flat electrodes could be extended to more complex electrodes, and beyond to 3D nanostructures. A few recently reported examples demonstrated the ability to transfer the determined molecular basis for DET from a planar to a more complex-structured electrode. The physicochemical properties of the SAM-modified gold electrodes obtained in the case of *M. verrucaria* BOD were transposed to functionalized nanoporous gold [197], as well as to functionalized carbon nanotubes films [30]. The requirement of an aromatic linker to anchor LAC via the Cu T1 was confirmed on films made of gold nanoparticles [198]. Catalysis with *A. aeolicus* Hase immobilized on carbon nanotubes presenting different surface chemistry highlighted good correlation with catalytic currents observed on the corresponding SAM functionality on planar gold electrodes. Agreement between the magnitudes of the catalytic current as a function of the surface chemistry on the carbon nanotubes with theoretical modeling of the dipole moment of the enzyme was also

demonstrated [194]. Nevertheless, only a low percentage, around 10%, of the loaded enzymes were electrically connected in the 3D structure [21], which suggests that other parameters than a correct enzyme orientation for DET drive catalysis in 3D conductive structures. One should be aware of the heterogeneity of electrochemical interfaces such as those formed by carbon nanotubes or carbon particles. Indeed, on such surfaces the walls of the carbon nanotubes are hydrophobic. Chemical functions are created upon carbon nanotube oxidative treatment or after π-binding of aromatic derivatives, yielding surfaces presenting various functionalities. The multiporosity displayed by 3D conductive surface must also be taken into account. Such a property is expected to be suitable for electrocatalysis, with macroporosity (pore diameter more than 50 nm) allowing fast substrate transport and mesoporosity allowing stable enzyme encapsulation. In the case when the pore is of the same dimension as the enzyme, one can expect that electrical connection of the enzyme might be efficient independently of its orientation, with the functionalities on the material serving only for stable anchorage [199]. In this case, however, transport processes should play a key role, both to provide a sufficient level of substrate to the enzyme and to permit fast evacuation of the product to avoid enzyme inhibition. This means that efficient bioelectrocatalysis will be achieved through a balance between electrical connection of a high amount of redox enzymes, protection of the enzymes in a suitable conductive structure, and substrate availability.

Acknowledgments: This work was supported by ANR (ENZYMOR-ANR-16-CE05-0024) and by the "Initiative d'Excellence" program from the French State (Grant "DYNAMO", ANR-11-LABX-0011-01).

Conflicts of Interest: The authors declare no conflict of interest.

References

1. Mellor, S.B.; Vavitsas, K.; Nielsen, A.Z.; Jensen, P.E. Photosynthetic fuel for heterologous enzymes: The role of electron carrier proteins. *Photosynth. Res.* **2017**, *134*, 329–342. [CrossRef] [PubMed]
2. Ilbert, M.; Bonnefoy, V. Insight into the evolution of the iron oxidation pathways. *Biochim. Biophys. Acta Bioenerg.* **2013**, *1827*, 161–175. [CrossRef] [PubMed]
3. Guiral, M.; Aussignargues, C.; Prunetti, L.; Infossi, P.; Ilbert, M.; Giudici-Orticoni, M.T. The energy sulfur metabolism of the hyperthermophilic bacterium *Aquifex aeolicus*. *Biochim. Biophys. Acta Bioenerg.* **2012**, *1817*, S155. [CrossRef]
4. Moehlenbrock, M.J.; Minteer, S.D. Extended lifetime biofuel cells. *Chem. Soc. Rev.* **2008**, *37*, 1188–1196. [CrossRef] [PubMed]
5. Maduraiveeran, G.; Sasidharan, M.; Ganesan, V. Electrochemical sensor and biosensor platforms based on advanced nanomaterials for biological and biomedical applications. *Biosens. Bioelectron.* **2018**, *103*, 113–129. [CrossRef] [PubMed]
6. Justino, C.I.L.; Duarte, A.C.; Rocha-Santos, T.A.P. Recent Progress in Biosensors for Environmental Monitoring: A review. *Sensors* **2017**, *17*, 2918. [CrossRef] [PubMed]
7. Clark, L.C.; Lyons, C. Electrode systems for continuous monitoring in cardiovascular surgery. *Ann. N. Y. Acad. Sci.* **1962**, *102*, 29–45. [CrossRef] [PubMed]
8. Bandodkar, A.J.; Imani, S.; Nunez-Flores, R.; Kumar, R.; Wang, C.Y.; Mohan, A.M.V.; Wang, J.; Mercier, P.P. Re-usable electrochemical glucose sensors integrated into a smartphone platform. *Biosens. Bioelectron.* **2018**, *101*, 181–187. [CrossRef] [PubMed]
9. Bruen, D.; Delaney, C.; Florea, L.; Diamond, D. Glucose Sensing for Diabetes Monitoring: Recent Developments. *Sensors* **2017**, *17*, 1866. [CrossRef] [PubMed]
10. Bandodkar, A.J.; Wang, J. Non-invasive wearable electrochemical sensors: A review. *Trends Biotechnol.* **2014**, *32*, 363–371. [CrossRef] [PubMed]
11. Santharaman, P.; Venkatesh, K.A.; Vairamani, K.; Benjamin, A.R.; Sethy, N.K.; Bhargava, K.; Karunakaran, C. ARM-microcontroller based portable nitrite electrochemical analyzer using cytochrome *c* reductase biofunctionalized onto screen printed carbon electrode. *Biosens. Bioelectron.* **2017**, *90*, 410–417. [CrossRef] [PubMed]

12. Huang, Y.; Tan, J.; Cui, L.J.; Zhou, Z.D.; Zhou, S.F.; Zhang, Z.H.; Zheng, R.; Xue, Y.W.; Zhang, M.X.; Li, S.S.; et al. Graphene and Au NPs co-mediated enzymatic silver deposition for the ultrasensitive electrochemical detection of cholesterol. *Biosens. Bioelectron.* **2018**, *102*, 560–567. [CrossRef] [PubMed]
13. Jakhar, S.; Pundir, C.S. Preparation, characterization and application of urease nanoparticles for construction of an improved potentiometric urea biosensor. *Biosens. Bioelectron.* **2018**, *100*, 242–250. [CrossRef] [PubMed]
14. Anik, U.; Tepeli, Y.; Diouani, M.F. Fabrication of Electrochemical Model Influenza A Virus Biosensor Based on the Measurements of Neuroaminidase Enzyme Activity. *Anal. Chem.* **2016**, *88*, 6151–6153. [CrossRef] [PubMed]
15. Sharma, B.; Dangi, A.K.; Shukla, P. Contemporary enzyme based technologies for bioremediation: A review. *J. Environ. Manag.* **2018**, *210*, 10–22. [CrossRef] [PubMed]
16. Morrison, C.S.; Armiger, W.B.; Dodds, D.R.; Dordick, J.S.; Koffas, M.A.G. Improved strategies for electrochemical 1,4-NAD(P)H_2 regeneration: A new era of bioreactors for industrial biocatalysis. *Biotechnol. Adv.* **2018**, *36*, 120–131. [CrossRef] [PubMed]
17. Bajracharya, S.; Srikanth, S.; Mohanakrishna, G.; Zacharia, R.; Strik, D.; Pant, D. Biotransformation of carbon dioxide in bioelectrochemical systems: State of the art and future prospects. *J. Power Sources* **2017**, *356*, 256–273. [CrossRef]
18. Hadj-Said, J.; Pandelia, M.E.; Leger, C.; Fourmond, V.; Dementin, S. The Carbon Monoxide Dehydrogenase from Desulfovibrio vulgaris. *Biochim. Biophys. Acta Bioenerg.* **2015**, *1847*, 1574–1583. [CrossRef] [PubMed]
19. Gamella, M.; Koushanpour, A.; Katz, E. Biofuel cells—Activation of micro- and macro-electronic devices. *Bioelectrochemistry* **2018**, *119*, 33–42. [CrossRef] [PubMed]
20. Mazurenko, I.; Wang, X.; de Poulpiquet, A.; Lojou, E. H_2/O_2 enzymatic fuel cells: From proof-of-concept to powerful devices. *Sustain. Energy Fuels* **2017**, *1*, 1475–1501. [CrossRef]
21. Mazurenko, I.; Monsalve, K.; Infossi, P.; Giudici-Orticoni, M.T.; Topin, F.; Mano, N.; Lojou, E. Impact of substrate diffusion and enzyme distribution in 3D-porous electrodes: A combined electrochemical and modelling study of a thermostable H_2/O_2 enzymatic fuel cell. *Energy Environ. Sci.* **2017**, *10*, 1966–1982. [CrossRef]
22. Hoarau, M.; Badieyan, S.; Marsh, E.N.G. Immobilized enzymes: Understanding enzyme—Surface interactions at the molecular level. *Org. Biomol. Chem.* **2017**, *15*, 9539–9551. [CrossRef] [PubMed]
23. Winkler, J.R.; Gray, H.B. Electron flow through metalloproteins. *Chem. Rev.* **2013**, *114*, 3369–3380. [CrossRef] [PubMed]
24. Marcus, R.A.; Sutin, N. Electron transfers in chemistry and biology. *Biochim. Biophys. Acta* **1985**, *811*, 265–322. [CrossRef]
25. Moser, C.C.; Keske, J.M.; Warncke, K.; Farid, R.S.; Dutton, P.L. Nature of biological electron-transfer. *Nature* **1992**, *355*, 796–802. [CrossRef] [PubMed]
26. Bostick, C.D.; Mukhopadhyay, S.; Pecht, I.; Sheves, M.; Cahen, D.; Lederman, D. Protein bioelectronics: A review of what we do and do not know. *Rep. Prog. Phys.* **2018**, *81*, 026601. [CrossRef] [PubMed]
27. Page, C.C.; Moser, C.C.; Chen, X.X.; Dutton, P.L. Natural engineering principles of electron tunnelling in biological oxidation-reduction. *Nature* **1999**, *402*, 47–52. [CrossRef] [PubMed]
28. Ozboyaci, M.; Kokh, D.B.; Corni, S.; Wade, R.C. Modeling and simulation of protein-surface interactions: Achievements and challenges. *Q. Rev. Biophys.* **2016**, *49*, e4. [CrossRef] [PubMed]
29. Léger, C.; Bertrand, P. Direct electrochemistry of redox enzymes as a tool for mechanistic studies. *Chem. Rev.* **2008**, *108*, 2379–2438. [CrossRef] [PubMed]
30. Mazurenko, I.; Monsalve, K.; Rouhana, J.; Parent, P.; Laffon, C.; Goff, A.L.; Szunerits, S.; Boukherroub, R.; Giudici-Orticoni, M.-T.; Mano, N. How the intricate interactions between carbon nanotubes and two bilirubin oxidases control direct and mediated O_2 reduction. *ACS Appl. Mater. Interfaces* **2016**, *8*, 23074–23085. [CrossRef] [PubMed]
31. Oteri, F.; Baaden, M.; Lojou, E.; Sacquin-Mora, S. Multiscale simulations give insight into the hydrogen in and out pathways of [NiFe]-hydrogenases from *Aquifex aeolicus* and Desulfovibrio fructosovorans. *J. Phys. Chem. B* **2014**, *118*, 13800–13811. [CrossRef] [PubMed]
32. Ogorzalek, T.L.; Wei, S.; Liu, Y.; Wang, Q.; Brooks, C.L., III; Chen, Z.; Marsh, E.N.G. Molecular-level insights into orientation-dependent changes in the thermal stability of enzymes covalently immobilized on surfaces. *Langmuir* **2015**, *31*, 6145–6153. [CrossRef] [PubMed]

33. Mano, N.; de Poulpiquet, A. O_2 Reduction in Enzymatic Biofuel Cells. *Chem. Rev.* **2018**, *118*, 2392–2468. [CrossRef] [PubMed]
34. Sakurai, T.; Kataoka, K. Basic and applied features of multicopper oxidases, CueO, bilirubin oxidase, and laccase. *Chem. Rec.* **2007**, *7*, 220–229. [CrossRef] [PubMed]
35. Solomon, E.I.; Augustine, A.J.; Yoon, J. O_2 Reduction to H_2O by the multicopper oxidases. *Dalton Trans.* **2008**, *30*, 3921–3932. [CrossRef] [PubMed]
36. Lubitz, W.; Ogata, H.; Rüdiger, O.; Reijerse, E. Hydrogenases. *Chem. Rev.* **2014**, *114*, 4081–4148. [CrossRef] [PubMed]
37. Fontecilla-Camps, J.C.; Volbeda, A.; Cavazza, C.; Nicolet, Y. Structure/function relationships of [NiFe]-and [FeFe]-hydrogenases. *Chem. Rev.* **2007**, *107*, 4273–4303. [CrossRef] [PubMed]
38. Wang, P.-H.; Best, R.B.; Blumberger, J. Multiscale simulation reveals multiple pathways for H_2 and O_2 transport in a [NiFe]-hydrogenase. *J. Am. Chem. Soc.* **2011**, *133*, 3548–3556. [CrossRef] [PubMed]
39. Wilson, R.; Turner, A. Glucose oxidase: An ideal enzyme. *Biosens. Bioelectron.* **1992**, *7*, 165–185. [CrossRef]
40. Hecht, H.; Schomburg, D.; Kalisz, H.; Schmid, R. The 3D structure of glucose oxidase from Aspergillus niger. Implications for the use of GOD as a biosensor enzyme. *Biosens. Bioelectron.* **1993**, *8*, 197–203. [CrossRef]
41. Zebda, A.; Gondran, C.; Le Goff, A.; Holzinger, M.; Cinquin, P.; Cosnier, S. Mediatorless high-power glucose biofuel cells based on compressed carbon nanotube-enzyme electrodes. *Nat. Commun.* **2011**, *2*, 370. [CrossRef] [PubMed]
42. Ludwig, R.; Ortiz, R.; Schulz, C.; Harreither, W.; Sygmund, C.; Gorton, L. Cellobiose dehydrogenase modified electrodes: Advances by materials science and biochemical engineering. *Anal. Bioanal. Chem.* **2013**, *405*, 3637–3658. [CrossRef] [PubMed]
43. Secundo, F. Conformational changes of enzymes upon immobilisation. *Chem. Soc. Rev.* **2013**, *42*, 6250–6261. [CrossRef] [PubMed]
44. Sugimoto, Y.; Kitazumi, Y.; Shirai, O.; Nishikawa, K.; Higuchi, Y.; Yamamoto, M.; Kano, K. Electrostatic roles in electron transfer from NiFe hydrogenase to cytochrome c_3 from Desulfovibrio vulgaris Miyazaki F. *Biochim. Biophys. Acta Proteins Proteom.* **2017**, *1865*, 481–487. [CrossRef] [PubMed]
45. Shimada, S.; Shinzawa-Itoh, K.; Baba, J.; Aoe, S.; Shimada, A.; Yamashita, E.; Kang, J.Y.; Tateno, M.; Yoshikawa, S.; Tsukihara, T. Complex structure of cytochrome *c*-cytochrome *c* oxidase reveals a novel protein-protein interaction mode. *EMBO J.* **2017**, *36*, 291–300. [CrossRef] [PubMed]
46. Kim, J.Y.; Kinoshita, M.; Kume, S.; Gt, H.; Sugiki, T.; Ladbury, J.E.; Kojima, C.; Ikegami, T.; Kurisu, G.; Goto, Y.; et al. Non-covalent forces tune the electron transfer complex between ferredoxin and sulfite reductase to optimize enzymatic activity. *Biochem. J.* **2016**, *473*, 3837–3854. [CrossRef] [PubMed]
47. Andralojc, W.; Hiruma, Y.; Liu, W.M.; Ravera, E.; Nojiri, M.; Parigi, G.; Luchinat, C.; Ubbink, M. Identification of productive and futile encounters in an electron transfer protein complex. *Proc. Natl. Acad. Sci. USA* **2017**, *114*, E1840–E1847. [CrossRef] [PubMed]
48. Kollipara, S.; Tatireddy, S.; Pathirathne, T.; Rathnayake, L.K.; Northrup, S.H. Contribution of Electrostatics to the Kinetics of Electron Transfer from NADH-Cytochrome b_5 Reductase to Fe(III)-Cytochrome b_5. *J. Phys. Chem. B* **2016**, *120*, 8193–8207. [CrossRef] [PubMed]
49. Cracknell, J.A.; Vincent, K.A.; Armstrong, F.A. Enzymes as working or inspirational electrocatalysts for fuel cells and electrolysis. *Chem. Rev.* **2008**, *108*, 2439–2461. [CrossRef] [PubMed]
50. Felder, C.E.; Prilusky, J.; Silman, I.; Sussman, J.L. A server and database for dipole moments of proteins. *Nucleic Acids Res.* **2007**, *35*, W512–W521. [CrossRef] [PubMed]
51. Topin, J.; Rousset, M.; Antonczak, S.; Golebiowski, J. Kinetics and thermodynamics of gas diffusion in a NiFe hydrogenase. *Proteins Struct. Funct. Bioinform.* **2012**, *80*, 677–682. [CrossRef] [PubMed]
52. Narth, C.; Gillet, N.; Cailliez, F.; Lévy, B.; de la Lande, A.L. Electron transfer, decoherence, and protein dynamics: Insights from atomistic simulations. *Acc. Chem Res.* **2015**, *48*, 1090–1097. [CrossRef] [PubMed]
53. Mazurenko, I.; de Poulpiquet, A.; Lojou, E. Recent developments in high surface area bioelectrodes for enzymatic fuel cells. *Curr. Opin. Electrochem.* **2017**, *5*, 74–84. [CrossRef]
54. Mazurenko, I.; Clément, R.; Byrne-Kodjabachian, D.; de Poulpiquet, A.; Tsujimura, S.; Lojou, E. Pore size effect of MgO-templated carbon on enzymatic H_2 oxidation by the hyperthermophilic hydrogenase from *Aquifex aeolicus*. *J. Electroanal. Chem.* **2018**, *812*, 221–226. [CrossRef]

55. Ash, P.A.; Liu, J.; Coutard, N.; Heidary, N.; Horch, M.; Gudim, I.; Simler, T.; Zebger, I.; Lenz, O.; Vincent, K.A. Electrochemical and Infrared Spectroscopic Studies Provide Insight into Reactions of the NiFe Regulatory Hydrogenase from Ralstonia eutropha with O_2 and CO. *J. Phys. Chem. B* **2015**, *119*, 13807–13815. [CrossRef] [PubMed]
56. Thorum, M.S.; Anderson, C.A.; Hatch, J.J.; Campbell, A.S.; Marshall, N.M.; Zimmerman, S.C.; Lu, Y.; Gewirth, A.A. Direct, Electrocatalytic Oxygen Reduction by Laccase on Anthracene-2-methanethiol-Modified Gold. *J. Phys. Chem. Lett.* **2010**, *1*, 2251–2254. [CrossRef] [PubMed]
57. Feng, G.; Niu, T.; You, X.; Wan, Z.; Kong, Q.; Bi, S. Studies on the effect of electrode pretreatment on the coverage of self-assembled monolayers of dodecanethiol on gold by electrochemical reductive desorption determination. *Analyst* **2011**, *136*, 5058–5063. [CrossRef] [PubMed]
58. Pankratov, D.; Sotres, J.; Barrantes, A.; Arnebrant, T.; Shleev, S. Interfacial behavior and activity of laccase and bilirubin oxidase on bare gold surfaces. *Langmuir* **2014**, *30*, 2943–2951. [CrossRef] [PubMed]
59. Trasatti, S.; Petrii, O. Real surface area measurements in electrochemistry. *Pure Appl. Chem.* **1991**, *63*, 711–734. [CrossRef]
60. Monsalve, K.; Roger, M.; Gutierrez-Sanchez, C.; Ilbert, M.; Nitsche, S.; Byrne-Kodjabachian, D.; Marchi, V.; Lojou, E. Hydrogen bioelectrooxidation on gold nanoparticle-based electrodes modified by *Aquifex aeolicus* hydrogenase: Application to hydrogen/oxygen enzymatic biofuel cells. *Bioelectrochemistry* **2015**, *106*, 47–55. [CrossRef] [PubMed]
61. Sezer, M.; Millo, D.; Weidinger, I.M.; Zebger, I.; Hildebrandt, P. Analyzing the catalytic processes of immobilized redox enzymes by vibrational spectroscopies. *IUBMB Life* **2012**, *64*, 455–464. [CrossRef] [PubMed]
62. Buividas, R.; Fahim, N.; Juodkazytė, J.; Juodkazis, S. Novel method to determine the actual surface area of a laser-nanotextured sensor. *Appl. Phys. A* **2014**, *114*, 169–175. [CrossRef]
63. Fang, S.-U.; Hsu, C.-L.; Hsu, T.-C.; Juang, M.-Y.; Liu, Y.-C. Surface roughness-correlated SERS effect on Au island-deposited substrate. *J. Electroanal. Chem.* **2015**, *741*, 127–133. [CrossRef]
64. Mendelsohn, R.; Mao, G.; Flach, C.R. Infrared Reflection-Absorption Spectroscopy: Principles and Applications to Lipid-Protein Interaction in Langmuir Films. *Biochim. Biophys. Acta* **2010**, *1798*, 788–800. [CrossRef] [PubMed]
65. Dongmo, S.; Wittstock, G.; Christoffers, J.; Brand, I. In situ determination of potential-driven structural changes in a redox-active plumbagin polymer film on a glassy carbon electrode using PM IRRAS under electrochemical control. *Electrochim. Acta* **2017**, *255*, 298–308. [CrossRef]
66. Heinz, H.; Vaia, R.; Farmer, B.; Naik, R. Accurate simulation of surfaces and interfaces of face-centered cubic metals using 12−6 and 9−6 Lennard-Jones potentials. *J. Phys. Chem. C* **2008**, *112*, 17281–17290. [CrossRef]
67. Iori, F.; Di Felice, R.; Molinari, E.; Corni, S. GolP: An atomistic force-field to describe the interaction of proteins with Au (111) surfaces in water. *J. Comput. Chem.* **2009**, *30*, 1465–1476. [CrossRef] [PubMed]
68. Heinz, H.; Lin, T.-J.; Kishore Mishra, R.; Emami, F.S. Thermodynamically consistent force fields for the assembly of inorganic, organic, and biological nanostructures: The INTERFACE force field. *Langmuir* **2013**, *29*, 1754–1765. [CrossRef] [PubMed]
69. Kubiak-Ossowska, K.; Jachimska, B.; Mulheran, P.A. How Negatively Charged Proteins Adsorb to Negatively Charged Surfaces: A Molecular Dynamics Study of BSA Adsorption on Silica. *J. Phys. Chem. B* **2016**, *120*, 10463–10468. [CrossRef] [PubMed]
70. Mücksch, C.; Urbassek, H.M. Molecular dynamics simulation of free and forced BSA adsorption on a hydrophobic graphite surface. *Langmuir* **2011**, *27*, 12938–12943. [CrossRef] [PubMed]
71. Trohalaki, S.; Pachter, R.; Luckarift, H.; Johnson, G. Immobilization of the Laccases from *Trametes versicolor* and *Streptomyces coelicolor* on Single-wall Carbon Nanotube Electrodes: A Molecular Dynamics Study. *Fuel Cells* **2012**, *12*, 656–664. [CrossRef]
72. Heinz, H.; Jha, K.C.; Luettmer-Strathmann, J.; Farmer, B.L.; Naik, R.R. Polarization at metal–biomolecular interfaces in solution. *J. R. Soc. Interface* **2011**, *8*, 220–232. [CrossRef] [PubMed]
73. Wright, L.B.; Rodger, P.M.; Corni, S.; Walsh, T.R. GolP-CHARMM: First-principles based force fields for the interaction of proteins with Au (111) and Au (100). *J. Chem. Theory Comput.* **2013**, *9*, 1616–1630. [CrossRef] [PubMed]
74. Shi, Y.; Xia, Z.; Zhang, J.; Best, R.; Wu, C.; Ponder, J.W.; Ren, P. Polarizable atomic multipole-based AMOEBA force field for proteins. *J. Chem. Theory Comput.* **2013**, *9*, 4046–4063. [CrossRef] [PubMed]

75. Akdim, B.; Pachter, R.; Kim, S.S.; Naik, R.R.; Walsh, T.R.; Trohalaki, S.; Hong, G.; Kuang, Z.; Farmer, B.L. Electronic properties of a graphene device with peptide adsorption: Insight from simulation. *ACS Appl. Mater. Interfaces* **2013**, *5*, 7470–7477. [CrossRef] [PubMed]
76. Datta, S.; Christena, L.R.; Rajaram, Y.R.S. Enzyme immobilization: An overview on techniques and support materials. *3 Biotech* **2013**, *3*, 1–9. [CrossRef] [PubMed]
77. Mohamad, N.R.; Marzuki, N.H.C.; Buang, N.A.; Huyop, F.; Wahab, R.A. An overview of technologies for immobilization of enzymes and surface analysis techniques for immobilized enzymes. *Biotechnol. Biotechnol. Equip.* **2015**, *29*, 205–220. [CrossRef] [PubMed]
78. Arya, S.K.; Prusty, A.K.; Singh, S.; Solanki, P.R.; Pandey, M.K.; Datta, M.; Malhotra, B.D. Cholesterol biosensor based on *N*-(2-aminoethyl)-3-aminopropyl-trimethoxysilane self-assembled monolayer. *Anal. Biochem.* **2007**, *363*, 210–218. [CrossRef] [PubMed]
79. Ulman, A. Formation and structure of self-assembled monolayers. *Chem. Rev.* **1996**, *96*, 1533–1554. [CrossRef] [PubMed]
80. Jin, B.; Wang, G.-X.; Millo, D.; Hildebrandt, P.; Xia, X.-H. Electric-field control of the pH-dependent redox process of cytochrome *c* immobilized on a gold electrode. *J. Phys. Chem. C* **2012**, *116*, 13038–13044. [CrossRef]
81. Bryant, M.A.; Crooks, R.M. Determination of surface pKa values of surface-confined molecules derivatized with pH-sensitive pendant groups. *Langmuir* **1993**, *9*, 385–387. [CrossRef]
82. Marmisollé, W.A.; Capdevila, D.A.; de la Llave, E.; Williams, F.J.; Murgida, D.H. Self-Assembled Monolayers of NH_2-Terminated Thiolates: Order, pK_a, and Specific Adsorption. *Langmuir* **2013**, *29*, 5351–5359. [CrossRef] [PubMed]
83. Gooding, J.J.; Ciampi, S. The molecular level modification of surfaces: From self-assembled monolayers to complex molecular assemblies. *Chem. Soc. Rev.* **2011**, *40*, 2704–2718. [CrossRef] [PubMed]
84. Dubois, L.H.; Nuzzo, R.G. Synthesis, structure, and properties of model organic surfaces. *Ann. Rev. Phys. Chem.* **1992**, *43*, 437–463. [CrossRef]
85. Love, J.C.; Estroff, L.A.; Kriebel, J.K.; Nuzzo, R.G.; Whitesides, G.M. Self-assembled monolayers of thiolates on metals as a form of nanotechnology. *Chem. Rev.* **2005**, *105*, 1103–1170. [CrossRef] [PubMed]
86. Schwartz, D.K. Mechanisms and kinetics of self-assembled monolayer formation. *Ann. Rev. Phys. Chem.* **2001**, *52*, 107–137. [CrossRef] [PubMed]
87. Porter, M.D.; Bright, T.B.; Allara, D.L.; Chidsey, C.E. Spontaneously organized molecular assemblies. 4. Structural characterization of n-alkyl thiol monolayers on gold by optical ellipsometry, infrared spectroscopy, and electrochemistry. *J. Am. Chem. Soc.* **1987**, *109*, 3559–3568. [CrossRef]
88. Jambrec, D.; Conzuelo, F.; Estrada-Vargas, A.; Schuhmann, W. Potential-Pulse-Assisted Formation of Thiol Monolayers within Minutes for Fast and Controlled Electrode Surface Modification. *ChemElectroChem* **2016**, *3*, 1484–1489. [CrossRef]
89. Samanta, D.; Sarkar, A. Immobilization of bio-macromolecules on self-assembled monolayers: Methods and sensor applications. *Chem. Soc. Rev.* **2011**, *40*, 2567–2592. [CrossRef] [PubMed]
90. Mondal, P.C.; Fontanesi, C. Electrochemistry of Metalloproteins Attached through Functional Self-Assembled Monolayers on Gold and Ferromagnetic Electrodes. *ChemPhysChem* **2018**, *19*, 60–66. [CrossRef] [PubMed]
91. Aydın, E.B.; Sezgintürk, M.K. Indium Tin Oxide (ITO): A promising material in biosensing technology. *TrAC Trends Anal. Chem.* **2017**, *97*, 309–315. [CrossRef]
92. Vashist, S.K.; Lam, E.; Hrapovic, S.; Male, K.B.; Luong, J.H. Immobilization of antibodies and enzymes on 3-aminopropyltriethoxysilane-functionalized bioanalytical platforms for biosensors and diagnostics. *Chem. Rev.* **2014**, *114*, 11083–11130. [CrossRef] [PubMed]
93. Yoshioka, K.; Kato, D.; Kamata, T.; Niwa, O. Cytochrome P450 modified polycrystalline indium tin oxide film as a drug metabolizing electrochemical biosensor with a simple configuration. *Anal. Chem.* **2013**, *85*, 9996–9999. [CrossRef] [PubMed]
94. Smalley, J.F.; Feldberg, S.W.; Chidsey, C.E.; Linford, M.R.; Newton, M.D.; Liu, Y.-P. The kinetics of electron transfer through ferrocene-terminated alkanethiol monolayers on gold. *J. Phys. Chem.* **1995**, *99*, 13141–13149. [CrossRef]
95. Xu, J.; Li, H.; Zhang, Y. Relationship between electronic tunneling coefficient and electrode potential investigated by using self-assembled alkanethiol monolayers on gold electrodes. *J. Phys. Chem.* **1993**, *97*, 11497–11500. [CrossRef]

96. Mokrani, C.; Fatisson, J.; Guerente, L.; Labbe, P. Structural characterization of (3-mercaptopropyl)sulfonate monolayer on gold surfaces. *Langmuir* **2005**, *21*, 4400–4409. [CrossRef] [PubMed]
97. Liu, B.; Bard, A.J.; Mirkin, M.V.; Creager, S.E. Electron transfer at self-assembled monolayers measured by scanning electrochemical microscopy. *J. Am. Chem. Soc.* **2004**, *126*, 1485–1492. [CrossRef] [PubMed]
98. Chi, Q.J.; Zhang, J.D.; Andersen, J.E.T.; Ulstrup, J. Ordered assembly and controlled electron transfer of the blue copper protein azurin at gold (111) single-crystal substrates. *J. Phys. Chem. B* **2001**, *105*, 4669–4679. [CrossRef]
99. Beulen, M.W.; Kastenberg, M.I.; van Veggel, F.C.; Reinhoudt, D.N. Electrochemical stability of self-assembled monolayers on gold. *Langmuir* **1998**, *14*, 7463–7467. [CrossRef]
100. Ovchinnikova, S.; Medvedev, A.Z. Desorption of octanethiol from gold electrode surface during its electrochemical cleaning. *Russ. J. Electrochem.* **2015**, *51*, 287–293. [CrossRef]
101. Stettner, J.; Winkler, A. Characterization of alkanethiol self-assembled monolayers on gold by thermal desorption spectroscopy. *Langmuir* **2010**, *26*, 9659–9665. [CrossRef] [PubMed]
102. Rzeźnicka, I.I.; Lee, J.; Maksymovych, P.; Yates, J.T. Nondissociative chemisorption of short chain alkanethiols on Au (111). *J. Phys. Chem. B* **2005**, *109*, 15992–15996. [CrossRef] [PubMed]
103. Ossowski, J.; Nascimbeni, G.; Żaba, T.; Verwüster, E.; Rysz, J.; Terfort, A.; Zharnikov, M.; Zojer, E.; Cyganik, P. Relative Thermal Stability of Thiolate-and Selenolate-Bonded Aromatic Monolayers on the Au (111) Substrate. *J. Phys. Chem. C* **2017**, *121*, 28031–28042. [CrossRef]
104. Wang, Y.; Solano Canchaya, J.G.; Dong, W.; Alcami, M.; Busnengo, H.F.; Martin, F. Chain-Length and Temperature Dependence of Self-Assembled Monolayers of Alkylthiolates on Au (111) and Ag (111) Surfaces. *J. Phys. Chem. A* **2014**, *118*, 4138–4146. [CrossRef] [PubMed]
105. Guo, L.; Ma, L.; Zhang, Y.; Cheng, X.; Xu, Y.; Wang, J.; Wang, E.; Peng, Z. Spectroscopic Identification of the Au–C Bond Formation upon Electroreduction of an Aryl Diazonium Salt on Gold. *Langmuir* **2016**, *32*, 11514–11519. [CrossRef] [PubMed]
106. Vacca, A.; Mascia, M.; Rizzardini, S.; Palmas, S.; Mais, L. Coating of gold substrates with polyaniline through electrografting of aryl diazonium salts. *Electrochim. Acta* **2014**, *126*, 81–89. [CrossRef]
107. Olejnik, P.; Palys, B.; Kowalczyk, A.; Nowicka, A.M. Orientation of laccase on charged surfaces. Mediatorless oxygen reduction on amino-and carboxyl-ended ethylphenyl groups. *J. Phys. Chem. C* **2012**, *116*, 25911–25918. [CrossRef]
108. Hetemi, D.; Pinson, J. Surface functionalisation of polymers. *Chem. Soc. Rev.* **2017**, *46*, 5701–5713. [CrossRef] [PubMed]
109. Santos, L.; Ghilane, J.; Lacroix, J.C. Formation of mixed organic layers by stepwise electrochemical reduction of diazonium compounds. *J. Am. Chem. Soc.* **2012**, *134*, 5476–5479. [CrossRef] [PubMed]
110. Santos, L.; Mattiuzzi, A.; Jabin, I.; Vandencasteele, N.; Reniers, F.O.; Reinaud, O.; Hapiot, P.; Lhenry, S.B.; Leroux, Y.; Lagrost, C. One-Pot Electrografting of Mixed Monolayers with Controlled Composition. *J. Phys. Chem. C* **2014**, *118*, 15919–15928. [CrossRef]
111. Leroux, Y.R.; Hapiot, P. Nanostructured monolayers on carbon substrates prepared by electrografting of protected aryldiazonium salts. *Chem. Mater.* **2013**, *25*, 489–495. [CrossRef]
112. Zhang, X.; Rösicke, F.; Syritski, V.; Sun, G.; Reut, J.; Hinrichs, K.; Janietz, S.; Rappich, J. Influence of the para-substitutent of benzene diazonium salts and the solvent on the film growth during electrochemical reduction. *Z. Phys. Chem.* **2014**, *228*, 557–573. [CrossRef]
113. Bouden, S.; Pinson, J.; Vautrin-Ul, C. Electrografting of diazonium salts: A kinetics study. *Electrochem. Commun.* **2017**, *81*, 120–123. [CrossRef]
114. Pita, M.; Gutierrez-Sanchez, C.; Olea, D.; Velez, M.; Garcia-Diego, C.; Shleev, S.; Fernandez, V.M.; De Lacey, A.L. High Redox Potential Cathode Based on Laccase Covalently Attached to Gold Electrode. *J. Phys. Chem. C* **2011**, *115*, 13420–13428. [CrossRef]
115. Alam, M.T.; Gooding, J.J. Modification of carbon electrode surfaces. In *Electrochemistry of Carbon Electrodes*; Wiley: Hoboken, NJ, USA, 2016; Volume 16.
116. Cracknell, J.A.; McNamara, T.P.; Lowe, E.D.; Blanford, C.F. Bilirubin oxidase from Myrothecium verrucaria: X-ray determination of the complete crystal structure and a rational surface modification for enhanced electrocatalytic O_2 reduction. *Dalton Trans.* **2011**, *40*, 6668–6675. [CrossRef] [PubMed]

117. Wiebalck, S.; Kozuch, J.; Forbrig, E.; Tzschucke, C.C.; Jeuken, L.J.C.; Hildebrandt, P. Monitoring the Transmembrane Proton Gradient Generated by Cytochrome bo_3 in Tethered Bilayer Lipid Membranes Using SEIRA Spectroscopy. *J. Phys. Chem. B* **2016**, *120*, 2249–2256. [CrossRef] [PubMed]
118. Wu, J.C.Y.; Hutchings, C.H.; Lindsay, M.J.; Werner, C.J.; Bundy, B.C. Enhanced enzyme stability through site-directed covalent immobilization. *J. Biotechnol.* **2015**, *193*, 83–90. [CrossRef] [PubMed]
119. Rueda, N.; dos Santos, J.; Ortiz, C.; Torres, R.; Barbosa, O.; Rodrigues, R.C.; Berenguer-Murcia, Á.; Fernandez-Lafuente, R. Chemical modification in the design of immobilized enzyme biocatalysts: Drawbacks and opportunities. *Chem. Rec.* **2016**, *16*, 1436–1455. [CrossRef] [PubMed]
120. Hibino, Y.; Kawai, S.; Kitazumi, Y.; Shirai, O.; Kano, K. Mutation of heme *c* axial ligands in D-fructose dehydrogenase for investigation of electron transfer pathways and reduction of overpotential in direct electron transfer-type bioelectrocatalysis. *Electrochem. Commun.* **2016**, *67*, 43–46. [CrossRef]
121. Balland, V.; Hureau, C.; Cusano, A.M.; Liu, Y.; Tron, T.; Limoges, B. Oriented Immobilization of a Fully Active Monolayer of Histidine-Tagged Recombinant Laccase on Modified Gold Electrodes. *Chemistry* **2008**, *14*, 7186–7192. [CrossRef] [PubMed]
122. Tsujimura, S.; Asahi, M.; Goda-Tsutsumi, M.; Shirai, O.; Kano, K.; Miyazaki, K. Direct electron transfer to a metagenome-derived laccase fused to affinity tags near the electroactive copper site. *Phys. Chem. Chem. Phys.* **2013**, *15*, 20585–20589. [CrossRef] [PubMed]
123. Li, Y.; Zhang, J.; Huang, X.; Wang, T. Construction and direct electrochemistry of orientation controlled laccase electrode. *Biochem. Biophys. Res. Commun.* **2014**, *446*, 201–205. [CrossRef] [PubMed]
124. Care, A.; Bergquist, P.L.; Sunna, A. Solid-binding peptides: Smart tools for nanobiotechnology. *Trends Biotechnol.* **2015**, *33*, 259–268. [CrossRef] [PubMed]
125. Shiba, K. Natural and artificial peptide motifs: Their origins and the application of motif-programming. *Chem. Soc. Rev.* **2010**, *39*, 117–126. [CrossRef] [PubMed]
126. Cui, Y.; Kim, S.N.; Jones, S.E.; Wissler, L.L.; Naik, R.R.; McAlpine, M.C. Chemical Functionalization of Graphene Enabled by Phage Displayed Peptides. *Nano Lett.* **2010**, *10*, 4559–4565. [CrossRef] [PubMed]
127. Nguyen, P.Q.; Botyanszki, Z.; Tay, P.K.R.; Joshi, N.S. Programmable biofilm-based materials from engineered curli nanofibres. *Nat. Commun.* **2014**, *5*, 4945. [CrossRef] [PubMed]
128. Hnilova, M.; Oren, E.E.; Seker, U.O.S.; Wilson, B.R.; Collino, S.; Evans, J.S.; Tamerler, C.; Sarikaya, M. Effect of Molecular Conformations on the Adsorption Behavior of Gold-Binding Peptides. *Langmuir* **2008**, *24*, 12440–12445. [CrossRef] [PubMed]
129. Khatayevich, D.; Gungormus, M.; Yazici, H.; So, C.; Cetinel, S.; Ma, H.; Jen, A.; Tamerler, C.; Sarikaya, M. Biofunctionalization of materials for implants using engineered peptides. *Acta Biomater.* **2010**, *6*, 4634–4641. [CrossRef] [PubMed]
130. Al-Lolage, F.A.; Meneghello, M.; Ma, S.; Ludwig, R.; Bartlett, P.N. A flexible method for the stable, covalent immobilization of enzymes at electrode surfaces. *ChemElectroChem* **2017**, *4*, 1528–1534. [CrossRef]
131. Lalaoui, N.M.; Rousselot-Pailley, P.; Robert, V.; Mekmouche, Y.; Villalonga, R.; Holzinger, M.; Cosnier, S.; Tron, T.; Le Goff, A. Direct electron transfer between a site-specific pyrene-modified laccase and carbon nanotube/gold nanoparticle supramolecular assemblies for bioelectrocatalytic dioxygen reduction. *ACS Catal.* **2016**, *6*, 1894–1900. [CrossRef]
132. Gao, X.; Ni, K.; Zhao, C.; Ren, Y.; Wei, D. Enhancement of the activity of enzyme immobilized on polydopamine-coated iron oxide nanoparticles by rational orientation of formate dehydrogenase. *J. Biotechnol.* **2014**, *188*, 36–41. [CrossRef] [PubMed]
133. Guan, D.; Kurra, Y.; Liu, W.; Chen, Z. A click chemistry approach to site-specific immobilization of a small laccase enables efficient direct electron transfer in a biocathode. *Chem. Commun.* **2015**, *51*, 2522–2525. [CrossRef] [PubMed]
134. Schlesinger, O.; Pasi, M.; Dandela, R.; Meijler, M.M.; Alfonta, L. Electron transfer rate analysis of a site-specifically wired copper oxidase. *Phys. Chem. Chem. Phys.* **2018**, *20*, 6159–6166. [CrossRef] [PubMed]
135. Johnson, D.L.; Martin, L.L. Controlling protein orientation at interfaces using histidine tags: An alternative to Ni/NTA. *J. Am. Chem. Soc.* **2005**, *127*, 2018–2019. [CrossRef] [PubMed]
136. Milton, R.D.; Minteer, S.D. Direct enzymatic bioelectrocatalysis: Differentiating between myth and reality. *J. R. Soc. Interface* **2017**, *14*. [CrossRef] [PubMed]
137. Marcus, R.A. Electron transfer reactions in chemistry. Theory and experiment. *Rev. Mod. Phys.* **1993**, *65*, 599. [CrossRef]

138. Lojou, E.; Cutruzzola, F.; Tegoni, M.; Bianco, P. Electrochemical study of the intermolecular electron transfer to *Pseudomonas aeruginosa* cytochrome cd_1 nitrite reductase. *Electrochim. Acta* **2003**, *48*, 1055–1064. [CrossRef]
139. Dos Santos, M.M.C.; de Sousa, P.M.P.; Goncalves, M.L.S.; Krippahl, L.; Moura, J.J.G.; Lojou, E.; Bianco, P. Electrochemical studies on small electron transfer proteins using membrane electrodes. *J. Electroanal. Chem.* **2003**, *541*, 153–162. [CrossRef]
140. Pedroso, H.A.; Silveira, C.M.; Almeida, R.M.; Almeida, A.; Besson, S.; Moura, I.; Moura, J.J.G.; Almeida, M.G. Electron transfer and docking between cytochrome cd_1 nitrite reductase and different redox partners—A comparative study. *Biochim. Biophys. Acta Bioenerg.* **2016**, *1857*, 1412–1421. [CrossRef] [PubMed]
141. Dagys, M.; Laurynėnas, A.; Ratautas, D.; Kulys, J.; Vidžiūnaitė, R.; Talaikis, M.; Niaura, G.; Marcinkevičienė, L.; Meškys, R.; Shleev, S. Oxygen electroreduction catalysed by laccase wired to gold nanoparticles via the trinuclear copper cluster. *Energy Environ. Sci.* **2017**, *10*, 498–502. [CrossRef]
142. Ciaccafava, A.; Infossi, P.; Ilbert, M.; Guiral, M.; Lecomte, S.; Giudici-Orticoni, M.T.; Lojou, E. Electrochemistry, AFM, and PM-IRRA Spectroscopy of Immobilized Hydrogenase: Role of a Hydrophobic Helix in Enzyme Orientation for Efficient H_2 Oxidation. *Angew. Chem. Int. Ed.* **2012**, *51*, 953–956. [CrossRef] [PubMed]
143. Rudiger, O.; Gutierrez-Sanchez, C.; Olea, D.; Pereira, I.A.C.; Velez, M.; Fernandez, V.M.; De Lacey, A.L. Enzymatic Anodes for Hydrogen Fuel Cells based on Covalent Attachment of Ni-Fe Hydrogenases and Direct Electron Transfer to SAM-Modified Gold Electrodes. *Electroanalysis* **2010**, *22*, 776–783. [CrossRef]
144. Vaz-Dominguez, C.; Pita, M.; de Lacey, A.L.; Shleev, S.; Cuesta, A. Combined ATR-SEIRAS and EC-STM Study of the Immobilization of Laccase on Chemically Modified Au Electrodes. *J. Phys. Chem. C* **2012**, *116*, 16532–16540. [CrossRef]
145. Gutierrez-Sanchez, C.; Ciaccafava, A.; Blanchard, P.Y.; Monsalve, K.; Giudici-Orticoni, M.T.; Lecomte, S.; Lojou, E. Efficiency of Enzymatic O_2 Reduction by Myrothecium verrucaria Bilirubin Oxidase Probed by Surface Plasmon Resonance, PMIRRAS, and Electrochemistry. *ACS Catal.* **2016**, *6*, 5482–5492. [CrossRef]
146. McArdle, T.; McNamara, T.P.; Fei, F.; Singh, K.; Blanford, C.F. Optimizing the Mass-Specific Activity of Bilirubin Oxidase Adlayers through Combined Electrochemical Quartz Crystal Microbalance and Dual Polarization Interferometry Analyses. *ACS Appl. Mater. Interfaces* **2015**, *7*, 25270–25280. [CrossRef] [PubMed]
147. Osawa, M.; Ataka, K.-I.; Yoshii, K.; Nishikawa, Y. Surface-Enhanced Infrared Spectroscopy: The Origin of the Absorption Enhancement and Band Selection Rule in the Infrared Spectra of Molecules Adsorbed on Fine Metal Particles. *Appl. Spectrosc.* **1993**, *47*, 1497–1502. [CrossRef]
148. Jiang, X.; Zaitseva, E.; Schmidt, M.; Siebert, F.; Engelhard, M.; Schlesinger, R.; Ataka, K.; Vogel, R.; Heberle, J. Resolving voltage-dependent structural changes of a membrane photoreceptor by surface-enhanced IR difference spectroscopy. *Proc. Natl. Acad. Sci. USA* **2008**, *105*, 12113–12117. [CrossRef] [PubMed]
149. Heidary, N.; Utesch, T.; Zerball, M.; Horch, M.; Millo, D.; Fritsch, J.; Lenz, O.; von Klitzing, R.; Hildebrandt, P.; Fischer, A.; et al. Orientation-controlled electrocatalytic efficiency of an adsorbed oxygen-tolerant hydrogenase. *PLoS ONE* **2015**, *10*, e0143101. [CrossRef] [PubMed]
150. Gutiérrez-Sanz, O.; Marques, M.; Pereira, I.A.C.; De Lacey, A.L.; Lubitz, W.; Rüdiger, O. Orientation and Function of a Membrane-Bound Enzyme Monitored by Electrochemical Surface-Enhanced Infrared Absorption Spectroscopy. *J. Phys. Chem. Lett.* **2013**, *4*, 2794–2798. [CrossRef]
151. Olejnik, P.; Pawłowska, A.; Pałys, B. Application of Polarization Modulated Infrared Reflection Absorption Spectroscopy for electrocatalytic activity studies of laccase adsorbed on modified gold electrodes. *Electrochim. Acta* **2013**, *110*, 105–111. [CrossRef]
152. Bergkvist, M.; Carlsson, J.; Oscarsson, S. A method for studying protein orientation with atomic force microscopy using relative protein volumes. *J. Phys. Chem. B* **2001**, *105*, 2062–2069. [CrossRef]
153. Traunsteiner, C.; Sek, S.; Huber, V.; Valero-Vidal, C.; Kunze-Liebhaeuser, J. Laccase immobilized on a mixed thiol monolayer on Au (111)—Structure-dependent activity towards oxygen reduction. *Electrochim. Acta* **2016**, *213*, 761–770. [CrossRef]
154. Gwyer, J.D.; Zhang, J.; Butt, J.N.; Ulstrupy, J. Voltammetry and in situ scanning tunneling microscopy of cytochrome *c* nitrite reductase on Au (111) electrodes. *Biophys. J.* **2006**, *91*, 3897–3906. [CrossRef] [PubMed]
155. Kartashov, A.V.; Serafini, G.; Dong, M.; Shipovskov, S.; Gazaryan, I.; Besenbacher, F.; Ferapontova, E.E. Long-range electron transfer in recombinant peroxidases anisotropically orientated on gold electrodes. *Phys. Chem. Chem. Phys.* **2010**, *12*, 10098–10107. [CrossRef] [PubMed]

156. Gutierrez-Sanchez, C.; Olea, D.; Marques, M.; Fernandez, V.M.; Pereira, I.A.C.; Velez, M.; De Lacey, A.L. Oriented Immobilization of a Membrane-Bound Hydrogenase onto an Electrode for Direct Electron Transfer. *Langmuir* **2011**, *27*, 6449–6457. [CrossRef] [PubMed]
157. Gutierrez-Sanz, O.; Natale, P.; Marquez, I.; Marques, M.C.; Zacarias, S.; Pita, M.; Pereira, I.A.C.; Lopez-Montero, I.; De Lacey, A.L.; Velez, M. H-2-Fueled ATP Synthesis on an Electrode: Mimicking Cellular Respiration. *Angew. Chem. Int. Ed.* **2016**, *55*, 6216–6220. [CrossRef] [PubMed]
158. Gutierrez-Sanz, O.; Olea, D.; Pita, M.; Batista, A.P.; Alonso, A.; Pereira, M.M.; Velez, M.; De Lacey, A.L. Reconstitution of Respiratory Complex I on a Biomimetic Membrane Supported on Gold Electrodes. *Langmuir* **2014**, *30*, 9007–9015. [CrossRef] [PubMed]
159. Matanovic, I.; Babanova, S.; Chavez, M.S.; Atanassov, P. Protein–Support Interactions for Rationally Designed Bilirubin Oxidase Based Cathode: A Computational Study. *J. Phys. Chem. B* **2016**, *120*, 3634–3641. [CrossRef] [PubMed]
160. Ngai, J.C.; Mak, P.-I.; Siu, S.W. ProtPOS: A python package for the prediction of protein preferred orientation on a surface. *Bioinformatics* **2016**, *32*, 2537–2538. [CrossRef] [PubMed]
161. Liu, J.; Yu, G.; Zhou, J. Ribonuclease A adsorption onto charged self-assembled monolayers: A multiscale simulation study. *Chem. Eng. Sci.* **2015**, *121*, 331–339. [CrossRef]
162. Kutzner, C.; Pall, S.; Fechner, M.; Esztermann, A.; de Groot, B.L.; Grubmuller, H. Best bang for your buck: GPU nodes for GROMACS biomolecular simulations. *J. Comput. Chem.* **2015**, *36*, 1990–2008. [CrossRef] [PubMed]
163. Salomon-Ferrer, R.; Case, D.A.; Walker, R.C. An overview of the Amber biomolecular simulation package. *Wiley Interdiscip. Rev. Comput. Mol. Sci.* **2013**, *3*, 198–210. [CrossRef]
164. Ponder, J.W.; Case, D.A. Force fields for protein simulations. *Adv. Protein Chem.* **2003**, *66*, 27–85. [PubMed]
165. Makrodimitris, K.; Masica, D.L.; Kim, E.T.; Gray, J.J. Structure prediction of protein−solid surface interactions reveals a molecular recognition motif of statherin for hydroxyapatite. *J. Am. Chem. Soc.* **2007**, *129*, 13713–13722. [CrossRef] [PubMed]
166. Xie, Y.; Zhou, J.; Jiang, S. Parallel tempering Monte Carlo simulations of lysozyme orientation on charged surfaces. *J. Chem. Phys.* **2010**, *132*, 02B602. [CrossRef] [PubMed]
167. Brancolini, G.; Kokh, D.B.; Calzolai, L.; Wade, R.C.; Corni, S. Docking of ubiquitin to gold nanoparticles. *ACS Nano* **2012**, *6*, 9863–9878. [CrossRef] [PubMed]
168. Zheng, J.; Li, L.; Chen, S.; Jiang, S. Molecular simulation study of water interactions with oligo (ethylene glycol)-terminated alkanethiol self-assembled monolayers. *Langmuir* **2004**, *20*, 8931–8938. [CrossRef] [PubMed]
169. Li, Y.; Ogorzalek, T.L.; Wei, S.; Zhang, X.; Yang, P.; Jasensky, J.; Brooks, C.L.; Marsh, E.N.G.; Chen, Z. Effect of immobilization site on the orientation and activity of surface-tethered enzymes. *Phys. Chem. Chem. Phys.* **2018**, *20*, 1021–1029. [CrossRef] [PubMed]
170. Cazelles, R.; Lalaoui, N.; Hartmann, T.; Leimkühler, S.; Wollenberger, U.; Antonietti, M.; Cosnier, S. Ready to use bioinformatics analysis as a tool to predict immobilisation strategies for protein direct electron transfer (DET). *Biosens. Bioelectron.* **2016**, *85*, 90–95. [CrossRef] [PubMed]
171. Utesch, T.; Millo, D.; Castro, M.A.; Hildebrandt, P.; Zebger, I.; Mroginski, M.A. Effect of the protonation degree of a self-assembled monolayer on the immobilization dynamics of a [NiFe] hydrogenase. *Langmuir* **2013**, *29*, 673–682. [CrossRef] [PubMed]
172. Oteri, F.; Ciaccafava, A.; De Poulpiquet, A.; Baaden, M.; Lojou, E.; Sacquin-Mora, S. The weak, fluctuating, dipole moment of membrane-bound hydrogenase from *Aquifex aeolicus* accounts for its adaptability to charged electrodes. *Phys. Chem. Chem. Phys.* **2014**, *16*, 11318–11322. [CrossRef] [PubMed]
173. Liu, J.; Xie, Y.; Peng, C.; Yu, G.; Zhou, J. Molecular Understanding of Laccase Adsorption on Charged Self-Assembled Monolayers. *J. Phys. Chem. B* **2017**, *121*, 10610–10617. [CrossRef] [PubMed]
174. Peng, L.; Utesch, T.; Yarman, A.; Jeoung, J.H.; Steinborn, S.; Dobbek, H.; Mroginski, M.A.; Tanne, J.; Wollenberger, U.; Scheller, F.W. Surface-Tuned Electron Transfer and Electrocatalysis of Hexameric Tyrosine-Coordinated Heme Protein. *Chemistry* **2015**, *21*, 7596–7602. [CrossRef] [PubMed]
175. Utesch, T.; Sezer, M.; Weidinger, I.M.; Mroginski, M.A. Adsorption of sulfite oxidase on self-assembled monolayers from molecular dynamics simulations. *Langmuir* **2012**, *28*, 5761–5769. [CrossRef] [PubMed]

176. Climent, V.; Zhang, J.; Friis, E.P.; Østergaard, L.H.; Ulstrup, J. Voltammetry and single-molecule in situ scanning tunneling microscopy of laccases and bilirubin oxidase in electrocatalytic dioxygen reduction on Au (111) single-crystal electrodes. *J. Phys. Chem. C* **2011**, *116*, 1232–1243. [CrossRef]
177. Madden, C.; Vaughn, M.D.; Díez-Pérez, I.; Brown, K.A.; King, P.W.; Gust, D.; Moore, A.L.; Moore, T.A. Catalytic turnover of [FeFe]-hydrogenase based on single-molecule imaging. *J. Am. Chem. Soc.* **2011**, *134*, 1577–1582. [CrossRef] [PubMed]
178. Xia, N.; Xing, Y.; Wang, G.; Feng, Q.; Chen, Q.; Feng, H.; Sun, X.; Liu, L. Probing of EDC/NHSS-mediated covalent coupling reaction by the immobilization of electrochemically active biomolecules. *Int. J. Electrochem. Sci.* **2013**, *8*, 2459–2467.
179. Palazon, F.; Montenegro Benavides, C.; Léonard, D.; Souteyrand, E.l.; Chevolot, Y.; Cloarec, J.-P. Carbodiimide/NHS derivatization of COOH-terminated SAMs: Activation or byproduct formation? *Langmuir* **2014**, *30*, 4545–4550. [CrossRef] [PubMed]
180. Ran, Q.; Peng, R.; Liang, C.; Ye, S.; Xian, Y.; Zhang, W.; Jin, L. Covalent immobilization of horseradish peroxidase via click chemistry and its direct electrochemistry. *Talanta* **2011**, *83*, 1381–1385. [CrossRef] [PubMed]
181. Singh, K.; McArdle, T.; Sullivan, P.R.; Blanford, C.F. Sources of activity loss in the fuel cell enzyme bilirubin oxidase. *Energy Environ. Sci.* **2013**, *6*, 2460–2464. [CrossRef]
182. Zanetti-Polzi, L.; Daidone, I.; Bortolotti, C.A.; Corni, S. Surface packing determines the redox potential shift of cytochrome *c* adsorbed on gold. *J. Am. Chem. Soc.* **2014**, *136*, 12929–12937. [CrossRef] [PubMed]
183. Krzemiński, Ł.; Cronin, S.; Ndamba, L.; Canters, G.W.; Aartsma, T.J.; Evans, S.D.; Jeuken, L.J.C. Orientational Control over Nitrite Reductase on Modified Gold Electrode and Its Effects on the Interfacial Electron Transfer. *J. Phys. Chem. B* **2011**, *115*, 12607–12614. [CrossRef] [PubMed]
184. Kakiuchi, T.; Iida, M.; Gon, N.; Hobara, D.; Imabayashi, S.-I.; Niki, K. Miscibility of adsorbed 1-undecanethiol and 11-mercaptoundecanoic acid species in binary self-assembled monolayers on Au (111). *Langmuir* **2001**, *17*, 1599–1603. [CrossRef]
185. Smith, R.K.; Reed, S.M.; Lewis, P.A.; Monnell, J.D.; Clegg, R.S.; Kelly, K.F.; Bumm, L.A.; Hutchison, J.E.; Weiss, P.S. Phase separation within a binary self-assembled monolayer on Au {111} driven by an amide-containing alkanethiol. *J. Phys. Chem. B* **2001**, *105*, 1119–1122. [CrossRef]
186. Benavidez, T.E.; Torrente, D.; Marucho, M.; Garcia, C.D. Adsorption of Soft and Hard Proteins onto OTCEs under the Influence of an External Electric Field. *Langmuir* **2015**, *31*, 2455–2462. [CrossRef] [PubMed]
187. Sugimoto, Y.; Kitazumi, Y.; Tsujimura, S.; Shirai, O.; Yamamoto, M.; Kano, K. Electrostatic interaction between an enzyme and electrodes in the electric double layer examined in a view of direct electron transfer-type bioelectrocatalysis. *Biosens. Bioelectron.* **2015**, *63*, 138–144. [CrossRef] [PubMed]
188. Sugimoto, Y.; Kitazumi, Y.; Shirai, O.; Yamamoto, M.; Kano, K. Role of 2-mercaptoethanol in direct electron transfer-type bioelectrocatalysis of fructose dehydrogenase at Au electrodes. *Electrochim. Acta* **2015**, *170*, 242–247. [CrossRef]
189. Lopez, F.; Siepenkoetter, T.; Xiao, X.; Magner, E.; Schuhmann, W.; Salaj-Kosla, U. Potential pulse-assisted immobilization of Myrothecium verrucaria bilirubin oxidase at planar and nanoporous gold electrodes. *J. Electroanal. Chem.* **2018**, *812*, 194–198. [CrossRef]
190. Millo, D.; Ranieri, A.; Gross, P.; Ly, H.K.; Borsari, M.; Hildebrandt, P.; Wuite, G.J.L.; Gooijer, C.; van der Zwan, G. Electrochemical Response of Cytochrome *c* Immobilized on Smooth and Roughened Silver and Gold Surfaces Chemically Modified with 11-Mercaptounodecanoic Acid. *J. Phys. Chem. C* **2009**, *113*, 2861–2866. [CrossRef]
191. Salewski, J.; Batista, A.P.; Sena, F.V.; Millo, D.; Zebger, I.; Pereira, M.M.; Hildebrandt, P. Substrate-Protein Interactions of Type II NADH:Quinone Oxidoreductase from Escherichia coli. *Biochemistry* **2016**, *55*, 2722–2734. [CrossRef] [PubMed]
192. Rivas, L.; Soares, C.M.; Baptista, A.M.; Simaan, J.; Di Paolo, R.E.; Murgida, D.H.; Hildebrandt, P. Electric-field-induced redox potential shifts of tetraheme cytochromes c_3 immobilized on self-assembled monolayers: Surface-enhanced resonance Raman spectroscopy and simulation studies. *Biophys. J.* **2005**, *88*, 4188–4199. [CrossRef] [PubMed]
193. Petrey, D.; Honig, B. Structural bioinformatics of the interactome. *Annu. Rev. Biophys.* **2014**, *43*, 193–210. [CrossRef] [PubMed]

194. Monsalve, K.; Mazurenko, I.; Gutierrez-Sanchez, C.; Ilbert, M.; Infossi, P.; Frielingsdorf, S.; Giudici-Orticoni, M.T.; Lenz, O.; Lojou, E. Impact of Carbon Nanotube Surface Chemistry on Hydrogen Oxidation by Membrane-Bound Oxygen-Tolerant Hydrogenases. *Chemelectrochem* **2016**, *3*, 2179–2188. [CrossRef]
195. Salamon, Z.; Fitch, J.; Cai, M.; Tumati, S.; Navratilova, E.; Tollin, G. Plasmon-waveguide resonance studies of ligand binding to integral proteins in membrane fragments derived from bacterial and mammalian cells. *Anal. Biochem.* **2009**, *387*, 95–101. [CrossRef] [PubMed]
196. Bouffier, L.; Doneux, T. Coupling electrochemistry with in situ fluorescence (confocal) microscopy. *Curr. Opin. Electrochem.* **2017**, *6*, 31–37. [CrossRef]
197. Siepenkoetter, T.; Salaj-Kosla, U.; Xiao, X.X.; Conghaile, P.O.; Pita, M.; Ludwig, R.; Magner, E. Immobilization of Redox Enzymes on Nanoporous Gold Electrodes: Applications in Biofuel Cells. *Chempluschem* **2017**, *82*, 553–560. [CrossRef]
198. Gutierrez-Sanchez, C.; Pita, M.; Vaz-Dominguez, C.; Shleev, S.; De Lacey, A.L. Gold Nanoparticles as Electronic Bridges for Laccase-Based Biocathodes. *J. Am. Chem. Soc.* **2012**, *134*, 17212–17220. [CrossRef] [PubMed]
199. Sugimoto, Y.; Kitazumi, Y.; Shirai, O.; Kano, K. Effects of Mesoporous Structures on Direct Electron Transfer-Type Bioelectrocatalysis: Facts and Simulation on a Three-Dimensional Model of Random Orientation of Enzymes. *Electrochemistry* **2017**, *85*, 82–87. [CrossRef]